HOKKAIDO UNIVERSITY

Title	Optical Study on Proximity Effect and Cooper Pair Recombination in Semiconductor Quantum Dots
Author(s)	Shabnam, Sinthia Mou
Citation	北海道大学. 博士(情報科学) 甲第12187号
Issue Date	2016-03-24
DOI	10.14943/doctoral.k12187
Doc URL	http://hdl.handle.net/2115/61707
Type	theses (doctoral)
File Information	Mou_Sinthia_Shabnam.pdf

Instructions for use

Hokkaido University Collection of Scholarly and Academic Papers : HUSCAP

Optical Study on Proximity Effect and Cooper Pair Recombination in Semiconductor Quantum Dots

December 2015

Sinthia Shabnam Mou

Graduate School of Information Science and Technology,
Hokkaido University, Japan

Laboratory of Nanophotonics
Research Institute for Electronic Science, Hokkaido University, Japan

Contents

Acknowledgement

The research work for this thesis has been carried out at the Laboratory of Nanophotonics, Research Institute for Electronic Science, Hokkaido University, Japan. I would like to express my most sincere gratitude and appreciation to Professor Ikuo Suemune for his continuous guidance, support and supervision throughout this entire work. I also would like to express my sincere gratitude to Professor Akihiro Murayama for supervising my work after April 2015. I would like to thank Prof. Hidekazu Kumano for his sincere support during my learning of the experimental works.

I sincerely thank Dr. Satoru Odashima and Dr. Hiroyuki Kurosawa for helping and assisting me through the sample fabrication process. I would like to thank Dr. Xiangming Liu and Dr. Hideaki Nakajima for helping me to learn the optical measurements.

I would like to thank Dr. Kouichi Akahane and Prof. Masahide Sasaki, of National Institute of Information and Communication Technology, Japan, for growing my semiconductor heterostructure sample wafer and Dr. Hiroshi Irie of NTT Basic Research Laboratories, Japan, for helping me with the deposition of Nb superconductor. I also thank Prof. Yasuhiro Asano for his assistance with some theoretical parts in this work. I express my thanks to all my co-workers for their support during accomplishing this thesis work.

Finally, I express my heartfelt gratitude and sincere thanks to my parents Prof. A. K. M. Ataur Rahman and Mrs. Parveen Akhtar, and my husband Muhammad Sajjadur Rahim, for their constant encouragement and kind support throughout this work.

Abstract

Spontaneous generation of quantum entangled photon pairs (QEPPs) has been actively studied for decades employing artificial atoms such as semiconductor quantum dots (QDs). However in comparison with the parametric down conversion (PDC) of incident photons via nonlinear optical medium, the simultaneous generation of photon pairs through the spontaneous recombination of electrons and holes in semiconductors has been difficult because of their mutual Coulomb interactions. In 2006, I. Suemune et al. proposed a new method to generate single QEPP at a time with Cooper-pair and hole-pair radiative recombination in a superconductor-based QD light emitting diode (SQLED). However, experimental studies of the Cooper-pair and hole-pair interactions in semiconductor QDs have not been performed.

In this thesis, I study luminescence properties of an n-typed-doped InAs QD heterostructure that is in close proximity with a niobium (Nb) superconductor in detail, with an objective to analyze the system's performance towards realizing the SQLED for generating QEPPs. The penetration and recombination of Cooper pairs in InAs QDs, below the superconducting (SC) critical temperature (T_C) of Nb, are experimentally demonstrated with photoluminescence (PL) spectroscopy of InAs-QD emission.

Ag/Nb-embedded nanopillars are fabricated with the InAs-QD-based heterostructure sample. I study luminescence spectra observed from InAs QDs embedded in the n-type InGaAs-based heterostructure, where electron Cooper pairs penetrate from the adjacent Nb superconductor with the proximity effect. At temperature below the SC T_C of Nb, substantial luminescence intensity enhancement is observed with continuous-wave (CW) and time-resolved PL spectroscopy. Based on these measurements, I study the Cooper-pair radiative recombination in InAs QDs and compare the measured results with those previously observed in quantum-well (QW) based SC-LEDs.

A sharp edge is observed in luminescence spectra of InAs QDs with the CW PL spectroscopy. I explain this result with the proximity effect, that is, with the consideration of opening of SC gap and the modification of density of states (DOS) near the electron Fermi level in the n-type semiconductor heterostructure. It is demonstrated that the sharp edge observed in the

QD luminescence spectra is well reproduced by including the SC-DOS, together with the quasiparticle lifetime broadening and the Gaussian distribution of lowest-QD-state emission lines. Based on these studies, I discuss the reason why it has been difficult with the previous QW-based SC-LEDs to observe this type of sharp edge that represents the SC-DOS in the luminescence spectra.

With temperature-dependent time-resolved QD luminescence measurements at the wavelength around 1570 nm, I observe shortening of the luminescence decay time constants at temperature below the SC T_C of Nb. This also confirms the Cooper-pair radiative recombination in InAs QDs observed with the CW measurements.

On the basis of the time-resolved PL measurements, I propose an analytical method to determine the contribution of Cooper-pair recombination in InAs QDs quantitatively. It is shown that the luminescence enhancement measured below SC T_C of Nb is well explained with the theory of Cooper-pair recombination, which is based on the second-order perturbation theory that deals with the electron-photon interaction. I also discuss the difference of the temperature-dependence of the Cooper-pair contribution between the present QD-based heterostructure samples and the previously measured QW-based LEDs.

All together, this thesis presents the detailed analytical studies and the discussion of the luminescence properties measured on the n-type InAs-QD-based heterostructure in close proximity with the Nb superconductor. This confirms the injection and recombination enhancement of Cooper pairs in InAs QDs. I believe this thesis is the firm one-step advancement towards realizing the proposed SQLED, for generating QEPPs.

Chapter 1

Introduction

1.1 Research Background:

With the ongoing advancement of information networks, information and communications technology is achieving more and more important roles in our community and society. The rapid growth of electronic commerce over the internet has led to an increasing demand for secure network communications. Quantum information and communications technology (Quantum ICT) is expected to provide the way for realizing efficient information processing [1] and secure information transmission [2] based on quantum mechanical principles. Quantum ICT offers the prospect of fundamentally secure communication by exploiting the fact that measurements of quantum systems unavoidably affect their states. This allows communicating agents to validate that there is no eavesdropper on the line [3]. Quantum Bits or "Qubits" are the basic information processing units of Quantum ICT, and their storage, processing, and transportation are the fundamental operations in such information networks [4]. The qubits are processed by coding and transferring the quantum states of nature's fastest and least-interacting particles: Photons. Since photon is a single quantum of light, it cannot be cloned [5] and this prevents eavesdropping in principle. Observation or measurement of photon's quantum state perturbs it and any attempts to eavesdrop during the photon transmission should instantaneously be detectable.

However, there remains an essential problem that photons can be eventually scattered or absorbed during their transmission through a quantum channel. This transmission loss limits the communication distances of single-photon-based quantum communication networks. For the expansion of such quantum networks to meet the global reach, development of quantum repeaters is necessary. Quantum teleportation and entanglement swapping based on quantum entanglement are expected to be one of the key tools to realize such quantum repeaters [6]. The idea is to divide a given long distance into shorter elementary links, employ initially independent quantum entanglement photon sources for each link, then create mutual quantum entanglement with the Bell-state measurements, thus extend the entanglement to the whole distance via entanglement swapping. In this regard, quantum entangled photon pair (QEPP)

sources play very important role in Quantum ICT. Quantum entanglement occurs when a two-photon state is not expressed by the direct product of the underlying states. Its interesting feature is that the two-photon states are correlated with each other but are not fixed until they are measured. One-photon state in the photon pair is fixed only when the other photon state is determined with measurements [7]. This property holds true regardless of how far the two photons are separated in space, which makes quantum teleportation and entanglement swapping appropriate for being employed in Quantum ICT.

Parametric down conversion (PDC) in an optical non-linear crystal has been widely used for sources to generate QEPPs [8, 9]. The pair generation rate of PDC has recently been dramatically improved, enabling an entanglement swapping at a telecom band at a practically sound rate [10]. In the PDC, however, the emission of multiple photon number components is unavoidable, which should increase a risk of eavesdropping in the application to quantum key distribution. Another drawback of the PDC is that the photon generation process is not deterministic but probabilistic, and in most cases, the experiments are made on the event selection basis for acquiring designated events, which makes the repetition rate of the operations slower and would complicate the synchronization between different device units in large-scale system integration. The on-demand generation of QEPPs with the regulated photon-number states is highly requested for quantum ICT applications, but it is yet to be realized and remains at a developing level.

The implementation of QEPP sources with solid-state devices has the potential for large-scale system integration as well as deterministic on-demand pair generation with nearly zero probabilities of multiple photon-number components. The method most frequently used is the biexciton-exciton cascaded emission of semiconductor quantum dots (QDs) [11 – 13]. The violation of Bell's inequality, which quantifies the high degree of entanglement [14], was demonstrated by a QD grown on a GaAs (001) substrate with temporal post-selection to reduce temporal gates [15]. It was also demonstrated by an isotropic QD grown with droplet epitaxy on a GaAs (111)A substrate [16]. However, demonstration of such a performance still remains difficult due to the fine structure splitting (FSS) of the exciton states for most QDs prepared with normal methods, which is induced mainly by their structural anisotropy [17].

Photons emitted from the biexciton-exciton cascade become energetically distinguishable by the FSS of the intermediate exciton states, and this prevents their entanglement. Biexciton–exciton cascade recombination processes also have a fundamental problem in generating ideal indistinguishable photon pairs. Because the lifetimes of the biexciton and exciton recombinations are generally different, the complete overlap of the two waveforms in the time scale is difficult to achieve. Cascade emission processes also result in a time difference between biexciton and exciton emissions, and the spin flip of the intermediate exciton states may occur during the time interval. This will induce decoherence between the two photon states. This is detrimental for photon qubit operations [4].

Instead of the cascaded photon emission, simultaneous two photon emission (TPE) method is preferable from the viewpoint of the little relative time delay and relative time jitter of the two photons for operations such as entanglement swapping. The TPE has been observed from atoms, such as hydrogen [18], but the emission rate is extremely low. It is also possible with semiconductors, but their TPE probability is five orders of magnitude weaker than the competitive one-photon emission [19], and the efficiency is quite low.

1.2 Purpose of This Work:

While various QEPP generation methods, e.g. parametric down conversion (PDC), biexciton-exciton cascaded emission, two photon emission (TPE), come with such limitations, I. Suemune et al. have proposed and have been working on a new possibility to generate on demand QEPP through conversion of electron Cooper pairs into entangled photon pairs via radiative recombination with a pair of normal holes in a superconductor based QD light emitting diode (SQLED) [4]. The theory is based on the injection of Cooper pairs from a superconducting electrode to an InGaAs-based heterostructure by the proximity effect. At a superconductor/normal-metal interface, Cooper pairs penetrate into the normal region by the proximity effect [20]. Electrons in superconductors form Cooper pairs which are spin-singlet entangled electron pairs [21]. The spin-singlet state of the Cooper pairs is free from the electron–hole exchange interaction, hence, when Cooper pairs are injected into a semiconductor QD, the strong electron-electron correlation of the Cooper pairs is expected to make it possible to recombine simultaneously with a pair of holes in the QD ground state to generate entangled photon pairs (EPPs) [4]. As Cooper pairs are bosons, the direct control of their number states is difficult [7]. This theory is based on the combination of the boson nature of the Cooper pairs and fermion nature of holes in the valence band of a QD. The number states of holes, in a single quantum state of the QD are limited by the Pauli's exclusion principle and a pair of holes forms the spin singlet state in the lowest state of the QD. This will regulate the number state of the entangled photon pairs generated by the recombination with the Cooper pairs.

I. Suemune and his group started their journey towards realizing their scheme of generating QEPP by fabricating an InGaAs-based superconducting (SC) light emitting diode (LED), where the n-type electrode was replaced with a niobium (Nb) superconductor electrode. The key issue of the SC LEDs is the proximity effect, where a normal metal in close proximity to a superconductor acquires SC properties, and its local density of states (DOS) is modified by the penetration of electron Cooper pairs. Experimentally, a normal metal surface that includes several SC islands was studied with scanning tunneling spectroscopy (STS) [22] and the proximity effect, especially spatial extension of the SC properties from the superconductor interface to the normal metal surface, was directly observed. Opening of the SC gap and the

modified SC DOS were observed on the normal-metal surface adjacent to the SC-island interface. Also, opening of the SC gap and the SC DOS induced in a semiconductor by the proximity effect was observed with InAs – Aluminum (Al) semiconductor-superconductor nanowires with tunneling spectroscopy [23].

In the experiments with SC-LEDs, drastic enhancement of luminescence at the wavelength of ~ 1.6 μm was observed below the superconducting critical temperature (T_C) of Nb [24]. The luminescence of a Cooper pair was analyzed with the second-order perturbation theory for the electron-photon interaction by Y. Asano et al., where a Cooper pair recombines with a pair of holes [25]. The theory predicted luminescence enhancement below Tc and it was demonstrated by I. Suemune et al. that the observed luminescence enhancement in SC-LEDs is well explained with the theory [26]. Sharp reduction of the LED luminescence decay time constant was also observed below T_C with another SC-LED which demonstrated a good agreement with the proposed theory of SQLED [27, 7]. These results evidenced the active role of Cooper pairs in radiative recombination in SC-LEDs.

However, SC-LEDs demonstrated in those previous works have been based on quantum well (QW) active regions. Although the predicted luminescence intensity enhancement was observed, any distinct variation of the luminescence spectra emitted from QW active layers of the SC LEDs could not be observed. The original proposal of the on-demand QEPP generation was based on a QD active layer [4]. When electrons near the electron Fermi level form spin-singlet Cooper pairs, they change from fermions to bosons of which number states are not fixed due to their coherent nature [7]. While Cooper pairs penetrate from the SC electrode into the semiconductor region, it is the minority holes, injected from the counter p-type electrode and populating the lowest-energy QD state in the valence band, that regulate the photon emission process. In this regard, I. Suemune et al. proposed to control the QEPP generation process by regulating the hole-number states via the valence-band lowest quantum state of a QD under the Pauli's exclusion principle [4].

In this work, I have studied the InAs QD-based semiconductor/Nb superconductor system in detail. I have analyzed luminescence of n-type doped InAs QD heterostructure in close

proximity to a Nb superconductor with CW and time-resolved luminescence measurements. The temperature dependence measurements showed abrupt enhancement of QD luminescence intensity below T_C of Nb which clearly confirmed penetration of Cooper pairs into QDs by the proximity effect and demonstrated SC effect in the luminescence of QDs. I have observed a sharp edge in luminescence spectra of InAs QDs at temperature below T_C. By studying the excitation power dependence of the observed sharp edge I have explained my observation with the proximity effect, considering the opening of SC gap and the SC DOS in the n-type semiconductor heterostructure, in which the QDs are embedded. I have also discussed the reason of absence of this sharp variation of luminescence spectra in the previous QW-based SC LEDs below and above T_C of Nb. With the help of time resolved measurements I have proposed a method to determine the contribution of Cooper-pair recombination without ambiguity. Based on these measurements and analysis, I have compared the properties of InAs QD-based semiconductor/superconductor system to the previously measured QW based SC-LEDs and discussed the difference between the properties of the two systems.

Therefore, the purpose of this thesis is the detailed study and discussion of the luminescence properties of n-typed doped InAs QD heterostructure in close proximity with Nb superconductor, with an objective to analyze the system's performance towards realizing superconductor based QD light emitting diode (SQLED) for generating quantum entangled photon pairs (QEPPs). This work also clarifies the difference between the previously studied luminescence of quantum well (QW) based superconducting light emitting diodes (SC-LEDs) and the Cooper pair luminescence in InAs QDs. Finally, from the detailed study and comparison, this thesis analyzes the progress and improvement in the system's performance after introducing QDs in the system, which will make situation approach towards realizing the proposed SQLED [4].

1.3 Each Chapter's Synopsis

The dissertation is assembled of five main chapters which discuss the background and concept of this research, sample preparation, measurement procedures and results of the performed measurements. The sixth chapter summarizes the work and presents an outlook of the future prospective. The details of the contents in each chapter are as follows:

- Chapter 1 introduces the background and objective of this work. It contains a brief discussion about the evolution and importance of quantum information and communication technology (ICT) in the current era and the role and application of quantum entangled photon pairs (QEPPs) in quantum ICT. It discusses about various methods, studied so far, for generation of EPPs and limitations of these methods. Finally the chapter introduces the new scheme for generating QEPPs employing Cooper pair recombination in InAs QDs, proposed by I. Suemune et al. [4]. It also discusses briefly about the works done so far for realizing this new proposed scheme. Based on the research background, the purpose of this thesis work is clarified in this chapter. In the last section this chapter provides the synopsis of each chapter in this thesis.

- Chapter 2 discusses and explains the concept of superconductor based QD light emitting diode (SQLED) in detail. It describes the working principle of the scheme in detail with appropriate figures, which includes the concept of SQLED fabrication, injection of Cooper pairs into QDs by proximity effect and Cooper pair – holes recombination process and the theory of QEPP generation. This chapter also reports the previous works which have been done with quantum well (QW) based superconducting light emitting diodes (SC-LEDs) with the aim of realizing the SQLED and discusses the overall advancement that have been made so far towards the realization of the scheme. Finally this chapter explains, in the light of the proposed theory by I. Suemune et al. [4], the importance of employing QD based heterostructure for realizing the scheme.

- Chapter 3 discusses the design and growth procedures of different layers of my experimental sample, that is, a heterostructure with InAs QDs embedded in n-type doped InGaAs. It describes the fabrication conditions maintained for different layers of the sample and presents

schematics that present the specifications of the fabricated layers and embedded QDs. This chapter also describes the step by step procedure of preparing the samples for optical measurements. It schematically explains the fabrication process of nanopillars on the sample with electron beam lithography and inductively coupled plasma reactive ion etching (ICP-RIE), deposition of Nb superconductor layer on the fabricated nanopillars and determination of the critical temperature (T_C) of the Nb layer deposited at the same time, deposition of thick Ag layer on the pillars with the Nb layer, and removal of the substrate to finally achieve Ag embedded pillars for improving extraction efficiency of generated photons. This chapter presents the schematic band structure of the prepared sample to explain the injection of Cooper pairs by the proximity effect and transportation of holes into QDs. In this chapter, I have also presented and discussed several reports on observation of opening of SC gap and modification of SC DOS in normal-metal and semiconductors by scanning tunneling spectroscopy (STS).

- Chapter 4 focuses on the photoluminescence (PL) spectroscopy of the prepared samples with continuous wave (CW) He-Ne excitation laser above and below T_C of the Nb superconductor. The first section of the chapter discusses the experimental setup for the measurements and the measurement procedure. The other two sections of this chapter present the optical properties obtained from the CW PL measurements and detailed analysis and discussion of those properties below and above T_C. The second section presents and discusses the luminescence spectra of the sample. It also presents the gradual temperature dependence of QD luminescence spectra and demonstrates abrupt enhancement of luminescence intensity below T_C which confirms SC effect in QD luminescence. In the third section of this chapter I have discussed the observed sharp edge in QD luminescence spectra below T_C in one of the prepared samples and explained this sharp feature with the proximity effect, that is, considering opening of SC gap and modification of density of states (DOS) near electron Fermi level in n-type doped semiconductor heterostructure. With quasiparticle lifetime broadening of the Cooper pairs and a Gaussian distribution of lowest QD state emission lines I demonstrated that the sharp edge luminescence spectra are well reproduced by the SC DOS.

- Chapter 5 presents the time resolved measurements of the Cooper pair recombination in InAs QDs. It discusses the experimental setup for the measurements and the measurement procedure. It presents the temperature and excitation power dependence of time-averaged QD luminescence spectra, transient luminescence peak intensity and luminescence decay time constant which demonstrate luminescence enhancement and reduction of luminescence decay time constants at temperature below T_C of Nb. This chapter also presents the analytical method and mathematical deductions which I used to calculate and determine the contribution of Cooper pair recombination in InAs QDs without ambiguity. Based on these measurements and with the help of the analytical method, I proposed a method to determine the contribution of Cooper-pair recombination in InAs QDs in this chapter. Later in this chapter, comparison was made between the temperature dependence of the ratio of superconductive to normal radiative recombination rate and the theoretical line obtained from the Cooper pair luminescence theory proposed in ref. 25, and the experimental data were fitted nicely with the theoretical curve and this confirmed the Cooper pair luminescence enhancement.

- The sixth chapter summarizes the whole work and concludes the observations and findings from the experimental results. Finally, based on the conclusions of this work this chapter presents an outlook of the future prospect.

References:

[1] J. L. O'Brien, A. Furusawa, and J. Vuckovic, Nat. Photon. 3, 687 (2009).

[2] N. Gisin, G. Ribordy, W. Tittel, and H. Zbinden, Rev. Mod. Phys. 74, 145 (2002).

[3] John J. L. Morton & Klaus MØlmer, Nature 153, vol. 517, 8 Jan 2015

[4] I. Suemune, T. Akazaki, K. Tanaka, M. Jo, K. Uesugi, M. Endo, H. Kumano, E. Hanamura, H. Takayanagi, M. Yamanishi, and H. Kan, Jpn. J. Appl. Phys. 45, 9264 (2006).

[5] W. K. Wooters and W. H. Zurek, Nature, vol. 299, pp. 802-803, Oct. 1982

[6] C. H. Bennett, G. Brassard, C. Crepeau, R. Jozsa, A. Peres, and W. K. Wootters, Phys. Rev. Lett. 70, 1895 (1993).

[7] I. Suemune, H. Sasakura, Y. Asano, H. Kumano, R. Inoue, K. Tanaka, T. Akazaki, and H. Takayanagi, IEICE Electron. Express 9, 1184 (2012).

[8] P. G. Kwiat, K. Mattle, H. Weinfurter, and A. Zeilinger, Phys. Rev. Lett. 75, 4337 (1995)

[9] C. K. Hong, Z. Y. Ou, and L. Mandel, Phys. Rev. Lett. 59, 2044 (1987).

[10] R. Jin, R. Shimizu, I. Morohashi, K. Wakui, M. Takeoka, S. Izumi, T. Sakamoto, M. Fujiwara, T. Yamashita, S. Miki, H. Terai, Z. Wang, and M. Sasaki, Sci. Rep. 4, 7468 (2014)

[11] C. L. Salter, R. M. Stevenson, I. Farrer, C. A. Nicoll, D. A. Ritchie, and A. J. Shields, Nature (London) 465, 594 (2010).

[12] A. Dousse, J. Suffczynski, A. Beveratos, O. Krebs, A. Lemaitre, I. Sagnes, J. Bloch, P. Voisin, and P. Senellart, Nature (London) 466, 217 (2010).

[13] M. Mueller, S. Bounouari, K. D. Joens, M. Glaessl, and P. Michler, Nat. Photon. 8, 224 (2014).

[14] W. J. Munro, K. Nemoto, and A. G. White, J. Mod. Opt. 48, 1239 (2001).

[15] R. J. Young, R. M. Stevenson, A. J. Hudson, C. A. Nicoll, D. A. Ritchie, and A. J. Shields, Phys. Rev. Lett. 102, 030406 (2009).

[16] T. Kuroda, T. Mano, N. Ha, H. Nakajima, H. Kumano, B. Urbaszek, M. Jo, M. Abbarchi, Y. Sakuma, K. Sakoda, I. Suemune, X.Marie, and T. Amand, Phys. Rev. B 88, 041306(R) (2013)

[17] A. J. Hudson, R. M. Stevenson, A. J. Bennett, R. J. Young, C. A. Nicoll, P. Atkinson, K. Cooper, D. A. Ritchie, and A. J. Shields, Phys. Rev. Lett. 99, 266802 (2007).

[18] G. Breit and E. Teller, Astrophys. J. 91, 215 (1940).

[19] A. Hayat, P. Ginzburg, and M. Orenstein, Nat. Photon. 2, 238 (2008).

[20] P. G. de Gennes, Superconductivity of Metals and Alloys (Boulder: Westview Press, 1999).

[21] L. Hofstetter, S. Csonka, J. Nygard, and C. Schoenenberger, Nature (London) 461, 960 (2009).

[22] L. Serrier-Garcia, J. C. Cuevas, T. Cren, C. Brun, V. Cherkez, F. Debontridder, D. Fokin, F. S. Bergeret, and D. Roditchev, Phys. Rev. Lett. 110, 157003 (2013).

[23] W. Chang, S. M. Albrecht, T. S. Jespersen, F. Kuemmeth, P. Krogstrup, J. Nyg°ard, and C. M. Marcus, Nat. Nanotechnol. 10, 232 (2015).

[24] Y. Hayashi, K. Tanaka, T. Akazaki, M. Jo, H. Kumano, and I. Suemune, Appl. Phys. Express 1, 011701 (2008)

[25] Y. Asano, I. Suemune, H. Takayanagi, and E. Hanamura, Phys. Rev. Lett. 103, 187001 (2009).

[26] I. Suemune, Y. Hayashi, S. Kuramitsu, K. Tanaka, T. Akazaki, H. Sasakura, R. Inoue, H. Takayanagi, Y. Asano, E. Hanamura, S. Odashima, and H. Kumano, Appl. Phys. Express 3, 054001 (2010).

[27] H. Sasakura, S. Kuramitsu, Y. Hayashi, K. Tanaka, T. Akazaki, E. Hanamura, R. Inoue, H. Takayanagi, Y. Asano, C. Hermannstaedter, H. Kumano, and I. Suemune, Phys. Rev. Lett. 107, 157403 (2011)

Chapter 2

Concept of Superconductor based Quantum Dot Light Emitting Diode (SQLED)

2.1 New Scheme for Generating QEPP

Spontaneous generation of quantum entangled photon pairs (QEPPs) has been actively studied for decades employing artificial atoms such as semiconductor quantum dots (QDs). But in comparison with the PDC of incident photons via nonlinear optical medium [1], the simultaneous generation of photon pairs through the spontaneous recombination of electrons and holes in semiconductors is difficult because of their mutual Coulomb interactions.

2.1.1 Special Aspect of Cooper Pair

In 2002, E. Hanamura made a unique proposal about the use of singlet states of Cooper pairs [2]. The injection of electron Cooper pairs and hole Cooper pairs into the same direct-band-gap medium via the proximity effect [3] is expected to induce the spontaneous recombination of electron- and hole-Cooper-pairs, which eventually results in the generation of entangled photon pairs. This unique feature of the Cooper-pair recombination has a potential to provide a process completely different from the biexciton–exciton cascade recombination.

The spin singlet states of the Cooper pairs have another advantage over the spin-splitting of the exciton state energies, which mainly originates from the QD potential anisotropy through the electron–hole exchange interactions [4]. As is generally known, the biexciton states are also spin singlet states and are free from electron–hole exchange interactions. The energy splitting of biexciton emission peaks frequently observed in photoluminescence (PL) spectra originates from the energy splitting of the exciton states, which are the final states for the biexciton transitions. The optical transitions related to the Cooper pairs are also free from the electron – hole exchange interactions and therefore the issue of exciton energy splitting [5].

On the other hand, since Cooper pairs are bosons, the control of the number states of photons generated by the optical transition is difficult. The generation of a single entangled photon pair at a time, which is the condition for the on-demand operation, with the injection of the Cooper pairs needs some additional control method.

2.1.2 Proposed Concept of SQLED

In 2006, I. Suemune et al. proposed a new method to generate single QEPP at a time with Cooper pair – holes radiative recombination in a superconductor based quantum-dot light emitting diode (SQLED) [5]. It is based on the control of the photon-pair generation process by the combination of the boson nature of the Cooper pairs and the fermion nature of holes. Since Cooper pairs are bosons and their number states are not fixed, the idea how to control the photon-pair generation process is to regulate the number of holes involved in the recombination with Cooper pairs. This is possible by the use of the ground state of the QD valence band that is under the Pauli's exclusion principle. This technique is expected to generate on QEPP.

The scheme can be realized by changing a conventional light emitting diode (LED) with a QD active medium in such a way that electron injection into the QDs is replaced with Cooper-pair injection. This could be done by replacing the n-type metal electrode of a normal LED with a superconductor. Cooper pairs induced in the superconductor electrode, below its superconducting critical temperature (T_C), are injected in the adjacent n-type semiconductor by the proximity effect through the Fermi level in the conduction band of QD [3]. During radiative recombination of Cooper pair – holes in a QD, the number of holes per pulsed excitation should be regulated definitely to two on the QD ground state energy level by the Pauli's exclusion principle. Then single QEPP generation is expected per excitation pulse. The fundamental device scheme and the operation of the SQLED will be described in the next section.

2.2 Device Structure and Fundamental Operation Conditions

A schematic of the fundamental SQLED and its relevant band structure is shown in Fig. 2.1. It is a conventional LED except for the n-type electrode replaced with a superconductor. Electron Cooper pairs are injected from the SC electrode into the n-type semiconductor via the proximity effect [3].

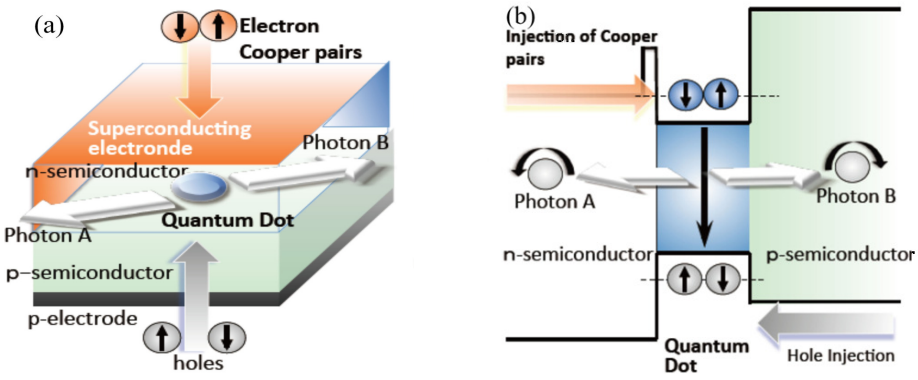

Fig. 2.1 Schematic of (a) SQLED and (b) the relevant band structure. Electron Cooper pairs are injected from the SC n-type electrode to a QD. The hole population in the valence QD state limits the recombination rate.

There are three crucial points that are needed to be considered for the successful operation of the device [6]. The first point is the Schottky barrier at the metal-semiconductor interface. The barrier height should be minimized for efficient injection. According to the Blonder–Tinkham–Klapwijk (BTK) theory [7], the supercurrent through a S–N junction is sensitively dependent on the tunnel barrier at the interface. In this simple model, a delta-functional barrier with the barrier height of Z was assumed and the results were critically dependent on the value of Z. In the proposed SQLED scheme by I. Suemune et al. [5], the S–Sm junction barrier height corresponding to Z is

the Schottky barrier at the metal – semiconductor interface. The conduction-band barrier height at metal/n-$In_xGa_{1-x}As$ interface is given by $\Delta E_C = 0.95 - 1.90x + 0.90x^2$ (eV) [8] and nonalloyed Ohmic contacts are possible for x ~ 0.8. Hence, In composition of x ≈ 0.8 makes reproducible Cooper-pair injection possible into the n- $In_xGa_{1-x}As$ [9].

The second important point is the thickness of the n-type semiconductor. It should be much less than the coherence length of the electron Cooper pairs penetrating into the n-type semiconductor [10, 11]. The proximity effect in n-type semiconductor is considered through a factor $e^{-2L_W/\xi_N(T)}$ [12], where $\xi_N(T) = \sqrt{\hbar D/2\pi T}$ is the coherence length in n-type region with $D = v_F^2\tau/3$ and τ being the diffusion constant and the elastic scattering relaxation time due to impurities, respectively. L_W is the thickness of n-type semiconductor. In the device structure proposed above (Fig. 2.1), the coherence length of the Cooper pairs penetrating into the n-InGaAs layer is estimated to be $\xi_N(T) = 1570\left[K^{\frac{1}{2}}\right]/\sqrt{T}$[nm] in the dirty limit which is much longer than the thickness of the n-InGaAs layer [10].

The third point is to make sure that the electron Cooper pairs can be efficiently injected to the conduction band of the QDs. The usual carrier injection scheme from adjacent barriers into a QD quantum state should not be applied in the present case, since injected carriers generally experience energy relaxations from the injected excited states to the QD ground state. The electron Cooper pairs injected into the n-type semiconductor are condensed near the Fermi level in the conduction band. The resonant injection of Cooper pairs into QD energy states is essentially important in this case, that is, the QD state should be tuned to the Fermi level for efficient tunneling of the Cooper pairs through thin potential barrier [5].

When the above mentioned points are realized, the electron Cooper pairs are evanescently injected into the conduction band of the QD from the n-type

semiconductor adjacent to the QD. Holes are injected into the QD lowest energy level through energy relaxation processes in the valence band from the adjacent p-type semiconductor, as shown in Fig. 2.1. The photon generation process is regulated by the population of holes. A pair of holes will occupy the lowest state in the QD valence band owing to the Pauli's exclusion principle and a hole spin singlet state will be eventually formed. The radiative recombination of the spin singlet electron Cooper pair and the hole pair will generate a circularly polarized photon pair. In this process, both the initial and final states are spin singlet, and the singlet states are free from the electron–hole exchange interactions. Therefore, this recombination process will be free from the QD anisotropy issue unlike the biexciton – exciton cascade recombination processes.

It is clear from the above discussion that the control of the number state of generated photon pairs is based on the Pauli's exclusion principle for the holes in the QD energy states. In conventional biexciton–exciton cascade photon-pair generations in a QD, a biexciton state is initially formed after every pulsed excitation with an appropriate intensity. The biexciton recombination generates a single photon from the QD, and the population in the QD is transferred to the exciton state, which eventually generates the counterpart photon and results in the cascade photon-pair generation [13, 14]. Therefore, for realizing on-demand single-photon-pair generations, the excitation pulse duration must be sufficiently short so that the QD will not be re-populated with biexcitons or excitons during the excitation. Similar operating conditions apply to the present SQ-LED, that is, the appropriate bias level to populate the valence-band QD state with a pair of holes that occupy the lowest QD state and the pulse duration short enough not to repopulate the valence-band QD states prior to the subsequent pulsed excitation [5].

2.3 Theoretical Expression of Cooper Pair Radiative Recombination

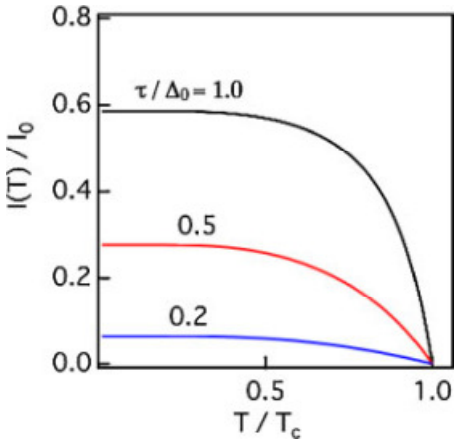

Fig. 2.2 Temperature dependence of theoretically calculated normalized luminescence intensity below the superconducting critical temperature (T_C) [9].

Figure 2.2 shows the luminescence intensity calculated with the relaxation time τ due to elastic impurity scattering. Δ_0 is half of the superconducting (SC) energy gap (pair potential) at zero temperature. The enhancement of the luminescence intensity for lowering the temperature below T_C is clearly visible in the figure, and the radiative recombination rate is analytically expressed in the following form [15, 9]:

$$W = \frac{1}{\tau_{rad,super}}$$
$$\approx |M|^4 N_0 \frac{\Delta^2(T)}{T} exp\left[-\frac{2L_W}{\xi_N(T)}\right] \sum_{q,\sigma} \frac{\tau}{\Gamma}$$
$$\equiv A \frac{\Delta^2(T)}{T} exp\left[-\frac{2L_W}{\xi_N(T)}\right] \quad (2.1)$$

Where $\tau_{rad,super}$ is the hole lifetime due to their radiative recombination with Cooper pairs in the active layer, M is the optical dipole transition amplitude, N_0 is the normal density of states in a superconductor at the Fermi energy, Δ(T) is the temperature dependent half of the SC energy gap, τ is the relaxation time related to the optical transitions and Γ is a more generalized relaxation term including the transfer process of Cooper pairs from the barrier layer to the active layer. The term $\exp[-2L_W/\xi_N(T)]$, as

already stated in the previous section of this chapter, is phenomenologically introduced to take the proximity effect into account where L_W is the distance from the S–Sm interface to the active layer and ξ_N is the coherence length of Cooper pairs in the normal medium (InGaAs semiconductor, in this case).

2.4 Previous Observations on Cooper Pair Radiative Recombination

Since the proposal of their new scheme to generate on demand QEPP through Cooper pair radiative recombination in a SQLED [5], I. Suemune and his group have been working on the practical realization of the scheme. Efficient injection of Cooper pairs into semiconductors was a prerequisite to realizing the proposed scheme, and for confirming Cooper pair injection capability, the group has been devoted to experiments with InGaAs-based superconducting light emitting diodes (SCLEDs) [16, 17].

In 2008, Y. Hayashi et al. experimentally examined and confirmed the contribution of cooper pairs in radiative recombination with holes in a semiconductor, by using a light emitting diode (LED) with a Nb superconductor electrode, where the electron cooper pairs were injected into the n-InGaAs active layer from the superconducting Nb electrode by the proximity effect [16]. Figure 2.3 shows the temperature dependence of the measured EL spectra of the experimental SCLED observed by Y. Hayashi et al.

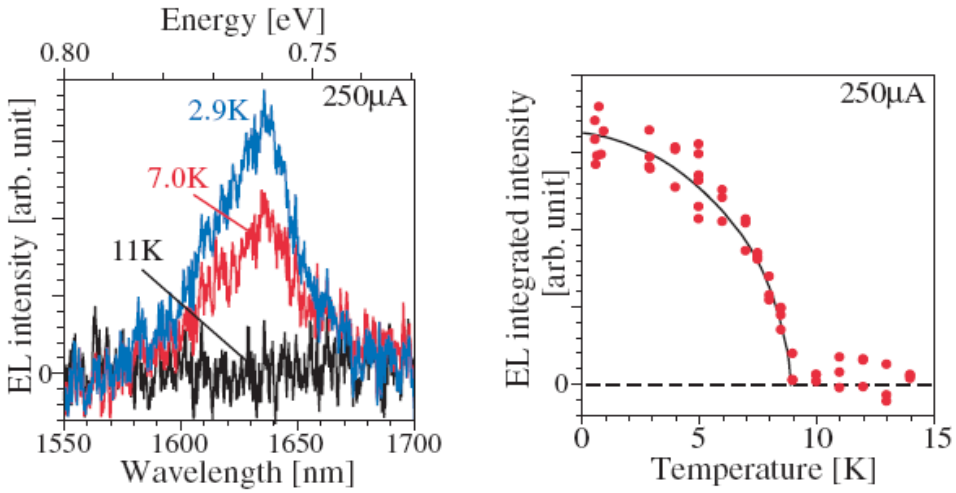

Fig. 2.3 Temperature dependence of (a) EL spectra and (b) EL integrated intensity where the solid line is guide to the eye. T_C of Nb ~ 8.4 K [16].

Drastic enhancement of the luminescence intensity at the temperature lower than the superconducting critical temperature (~ 8.4 K, in this case) is observed in Fig. 2.3, while at higher temperature the EL intensity remained at noise level. This drastic enhancement of the radiative recombinations in n-InGaAs semiconductor below T_C clearly evidences penetration of Cooper pairs in the semiconductor active layer.

In 2011, H Sasakura et al. experimentally demonstrated drastic enhancement of the radiative recombination rate in a semiconductor, due to involvement of Cooper pairs in the photon generation process [17]. Electron Cooper pairs injected from a superconducting electrode into an active layer by the proximity effect recombined with holes injected from a p-type electrode. The measured radiative decay time rapidly decreased with decreasing temperature below the superconducting critical temperature (T_C) of the niobium (Nb) electrodes, as shown in Fig. 2.4. The observation confirmed the role of Cooper pairs in radiative recombination in the prepared SC-LEDs.

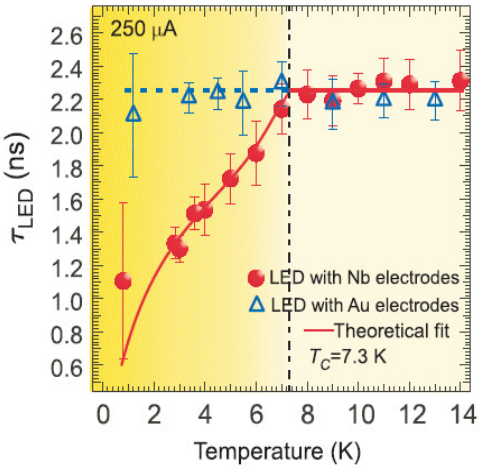

Fig. 2.4 Temperature dependence of the measured LED decay time, τ_{LED} [17].

2.5 Remaining Issue Towards Realizing SQLED

Both the observations referred in the previous section, that is, drastic enhancement of the luminescence intensity and sharp reduction of luminescence decay time constant below T_C of Nb, demonstrated Cooper pairs radiative recombination in semiconductor active layer. However, SC-LEDs demonstrated in those previous works were based on quantum well (QW) active regions. The original proposal of the on-demand QEPP generation in a SQLED, by I. Suemune et al., was based on a QD active region [5]. Cooper pairs are bosons and due to their coherent nature their number states are not fixed and are hard to control. In this regard, the photon emission from the SQLED is proposed to be regulated by minority holes populating the lowest-energy QD state in the valence band under the Pauli's exclusion principle.

The objective of my work, as a continuation of the journey towards realizing SQLED, is to study Cooper-pair recombination in n-typed doped InAs QD heterostructure in close proximity with Nb superconductor and to examine the relation of QD states and Cooper pair recombination. My aim is to analyze the QD based n-type semiconductor heterostructure system's performance towards realizing superconductor based QD light emitting diode (SQLED) for generating quantum entangled photon pairs (QEPPs).

References:

[1] P. G. Kwiat, K. Mattle, H. Weinfurter, A. Zeilinger, A. V. Sergienko and Y. Shih: Phys. Rev. Lett. 75 (1995) 4337.

[2] E. Hanamura: Phys. Status Solidi B 234 (2002) 166.

[3] P. G. de Gennes: Superconductivity of Metals and Alloys (Westview Press, ABP, Boulder, 1999)

[4] V. D. Kulakovskii, G. Bacher, R. Weigand, T. Kummell, A. Forchel, E. Borovitskaya, K. Leonardi and D. Hommel: Phys. Rev. Lett. 82 (1999) 1780.

[5] I. Suemune, T. Akazaki, K. Tanaka, M. Jo, K. Uesugi, M. Endo, H. Kumano, E. Hanamura, H. Takayanagi, M. Yamanishi, and H. Kan, Jpn. J. Appl. Phys., 45, 9264 (2006)

[6] S. S. Mou, H. Irie, Y. Asano, K. Akahane, H. Kurosawa, H. Nakajima, H. Kumano, M. Sasaki, and I. Suemune, IEEE J. Sel. Top. Quantum Electron. 21, 7900111 (2015)

[7] G. E. Blonder, M. Tinkham, and T. M. Klapwijk: Phys. Rev. B 25, 4515, (1982)

[8] K. Kajiyama, Y. Mizushima, and S. Sakata: Appl. Phys. Lett. 23, 458, (1973)

[9] I. Suemune, H. Sasakura, Y. Hayashi, K. Tanaka, T. Akazaki, Y. Asano, R. Inoue, H. Takayanagi, E. Hanamura, J.-H. Huh, C. Hermannstaedter, S. Odashima, and H. Kumano, Jpn. J. Appl. Phys., 51, 010114-1, (2012)

[10] I. Suemune, H. Sasakura, Y. Asano, H. Kumano, R. Inoue, K. Tanaka, T. Akazaki, and H. Takayanagi, IEICE Electron. Express, 9, 1184 (2012).

[11] H. Sasakura, S. Kuramitsu, Y. Hayashi, K. Tanaka, T. Akazaki, E. Hanamura, R. Inoue, H. Takayanagi, Y. Asano, C. Hermannstaedter, H. Kumano, and I. Suemune, Phys. Rev. Lett. 107, 157403 (2011)

[12] R. D. Parks, Superconductivity. New York, NY, USA: Marcel Dekker, 1969

[13] A. Kiraz, S. Falth, C. Becher, B. Gayral, W. V. Schoenfeld, P. M. Petroff, L. Zhang, E. Hu and A. Imamoglu: Phys. Rev. B 65, 161303, (2002)

[14] Z. Yuan, B. E. Kardynal, R. M. Stevenson, A. J. Shields, C. J. Lobo, K. Cooper, N. S. Beattie, D. A. Ritchie and M. Pepper: Science 295, 102, (2002)

[15] Y. Asano, I. Suemune, H. Takayanagi, and E. Hanamura, Phys. Rev. Lett. 103, 187001 (2009)

[16] Y. Hayashi, K. Tanaka, T. Akazaki, M. Jo, H. Kumano, and I. Suemune, Appl. Phys. Express 1, 011701 (2008)

[17] H. Sasakura, S. Kuramitsu, Y. Hayashi, K. Tanaka, T. Akazaki, E. Hanamura, R. Inoue, H. Takayanagi, Y. Asano, C. Hermannstaedter, H. Kumano, and I. Suemune, Phys. Rev. Lett. 107, 157403 (2011)

Chapter 3
Preparation of Sample

3.1 InAs Quantum Dot Heterostructure Grown on InP Substrate

The proposal of on-demand quantum entangled photon pair (QEPP) generation in a superconductor based quantum dot light emitting diode (SQLED), by I. Suemune et al., was based on the conversion of the Cooper pairs, which are entangled electron pairs, to QEPPs via the radiative recombination in a QD [1]. In this regard, with an objective to move forward towards realizing the SQLED, I have worked on an n-doped InAs-QD-based semiconductor heterostructure sample that is in close proximity with a Nb superconductor to study Cooper pair recombination in QDs.

As stated in the previous chapter (Chapter 2), SCLEDs, used in the past experiments for observing Cooper pair radiative recombination in the semiconductor active layer, had the active quantum well (QW) regions at the center of p-n junction [2, 3]. Without external bias, p-n junctions induce internal built-in potential and deplete the active layers. The depletion layer induced at the junction by the built-in potential prevents penetration of Cooper pairs into QDs located at the junction. Therefore, application of external bias changes both the potential profile near QDs and the current injection, and this makes the situation complex. On the other hand, uniform n-type doping keeps the electron Fermi level constant in the whole semiconductor structure and offers a simpler basis for the study of the proximity effect. Then, by injecting minority holes with an external optical excitation, a flow of supercurrent can be produced from the adjacent superconductor into InAs QDs and Cooper-pair luminescence will be generated. Based on this consideration, I used an n-type doped QD-based heterostructure sample for my experiments, which is schematically shown in Fig. 3.1 (a).

The sample was fabricated with molecular beam epitaxy (MBE) on an InP (311)B substrate. The reason for growing it on the InP (311)B substrate is that growth on usual InP (001) substrates tends to result in elongated quantum dashes instead of QDs [4]. The growth was started with the 50-nm-thick $In_{0.53}Ga_{0.47}As$/100-nm-thick $In_{0.52}Al_{0.48}As$ undoped layers, which are for the selective etching to remove the InP substrate later. Then, the growth was followed

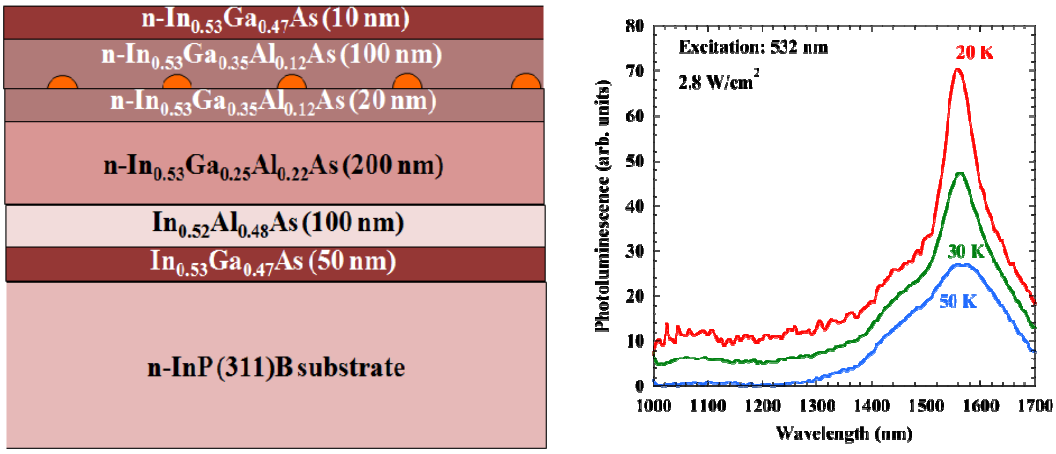

(a) (b)

Fig. 3.1 (a) Schematic of InAs QD-based heterostructure sample and **(b)** Photoluminescence (PL) spectra measured on the heterostructure.

by the heterostructure of 200-nm-thick n-$In_{0.53}Ga_{0.25}Al_{0.22}As$/20-nm-thick n-$In_{0.53}Ga_{0.35}Al_{0.12}As$ barrier layers, 5-monolayer of InAs QDs, and 100-nm-thick n-$In_{0.53}Ga_{0.35}Al_{0.12}As$ barrier layer. Finally a thin (10 nm) n-$In_{0.53}Ga_{0.47}As$ layer was grown on top of the surface for preparing ohmic contact to the superconducting Nb layer later.

The n-type doping level of the barrier layers was ~ $1x10^{18}$ cm^{-3}. The QDs layer was modulation doped from the adjacent n-type $In_{0.53}Ga_{0.35}Al_{0.12}As$ barriers. All the layers of the heterostructure was grown at 470 ºC, except for the QDs. The 5-monolayer of InAs QDs was grown at 530 ºC. The QDs grown on the (311)B crystal surface keep a circular shape, but the QD density is high, typically 9×10^{10} cm^{-2}, at 470°C. It was reduced to the density of 3.4×10^{10} cm^{-2} by increasing the temperature to 530 °C [5]. After the QDs growth, the substrate temperature was lowered to 470 °C again for the subsequent layers' growth. The sample's average QD lateral size and height were 57 and 5.6 nm, respectively.

Figure 3.1(b) shows the photoluminescence (PL) spectra measured on the heterostructure and it is observed that the QD emission dominates around 1580 nm (~ 785 meV).

3.2 Fabrication of Nanopillars

The sample surface, shown in Fig. 3.1 (a), was etched into a periodic array of pillars with different diameters ranging from 200 nm to 2 µm and the height ~ 700 nm. Figure 3.2 presents the steps of the pillar fabrication procedure.

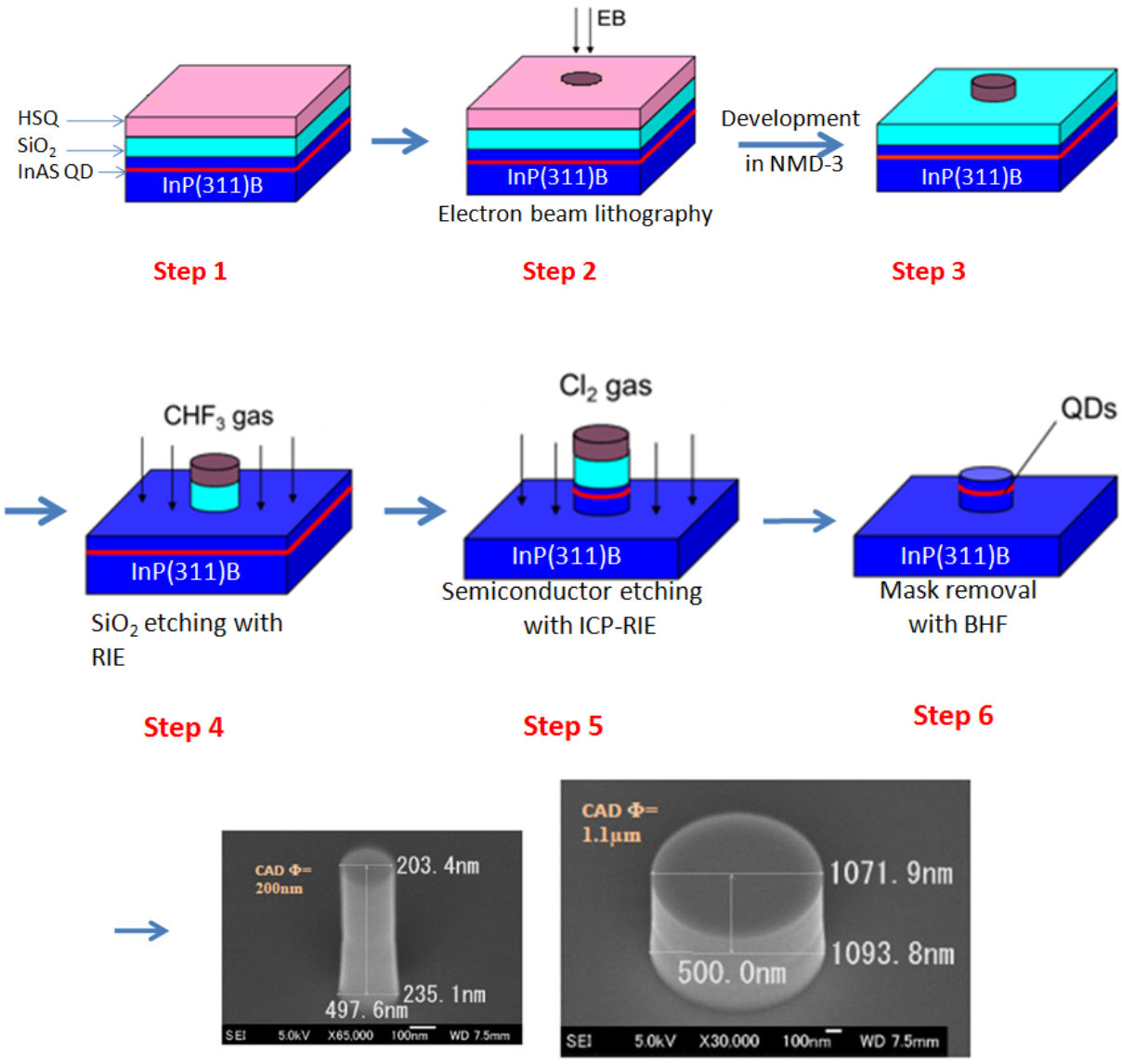

Fig. 3.2 Fabrication procedure of nanopillars.

As shown in Fig. 3.2, in the first step of pillar fabrication, the sample wafer is cleaved into pieces (5 mm x 5 mm, in my case) and 300 nm SiO_2 layer was deposited on the sample by plasma assisted chemical vapor deposition (PCVD) method. The SiO_2 layer helps stabilizing the adhesion of the electron-beam (e-beam) resist layer. Then coating of ~ 500-nm thick hydrogen silsequioxane (HSQ) resist layer is made on the sample by spin coating.

In step 2, the array of the pillars' pattern is drawn on the HSQ surface by e-beam lithography by exposing the sample with an e-beam which is programmed and customized by the desired computer aided design (CAD) pattern.

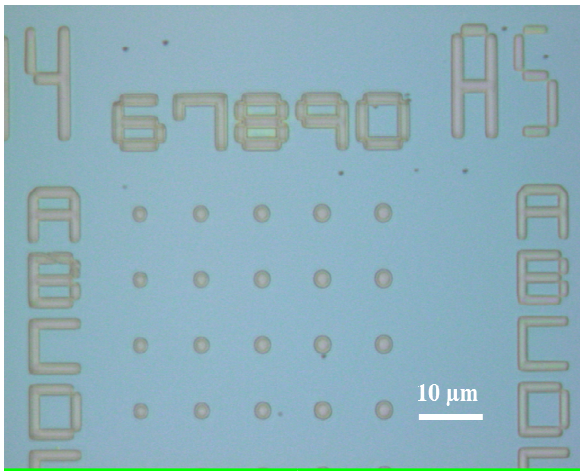

Fig. 3.3 Pillars pattern drawn on the sample by e-beam lithography.

After e-beam lithography, I developed the sample in NMD solution to remove the unwanted resist. Figure 3.3 shows the pillar patterns appeared on the sample surface after e-beam lithography and NMD developing.

Following the resist patterning, the sample is etched by Reactive Ion Etching (RIE) to remove the 300 nm thick SiO_2. Finally the pillars are etched by inductively coupled plasma reactive ion etching (ICP RIE) and the remaining mask (SiO_2 + HSQ) on the top of the pillars is removed by rinsing the sample in buffered Hydrofluoric Acid (HF) and then in pure water. The SEM images of as etched pillars are shown in the bottom of figure 3.2.

3.3 Deposition and Characterization of Nb Superconductor

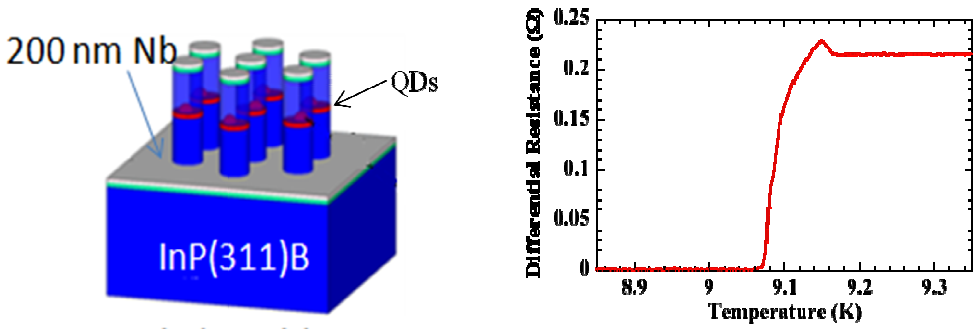

Fig. 3.4 (a) Deposition of Nb superconductor on the fabricated pillars and **(b)** Determination of the critical temperature (T_C) of the Nb layer.

After the fabrication of the nanopillars, 200 nm thick Nb superconductor layer was deposited on the as etched pillars by an e-beam evaporation method, as shown in Fig. 3.4 (a). The critical temperature (T_C) of the Nb superconductor was measured with a reference Nb sample, on which Nb was simultaneously evaporated on another piece of InP (311)B substrate in the same evaporation chamber. Figure 3.4 (b) shows the temperature dependence of the differential resistance of the evaporated Nb layer and the SC critical temperature T_C is ~ 9.09 K.

3.4 Ag Embedded Pillars

My next target was to observe the luminescence from the Nb-superconductor/InGaAs-based semiconductor heterostructure samples by the optical access from the backside through the InP substrate. But InP has the high refractive index of ~3.5 and the total internal reflection at an InP/air interface limits the photon extraction efficiency to below 2% [6]. To improve this low efficiency to a higher value, Nb based metal-embedded semiconductor pillar structures were fabricated [7].

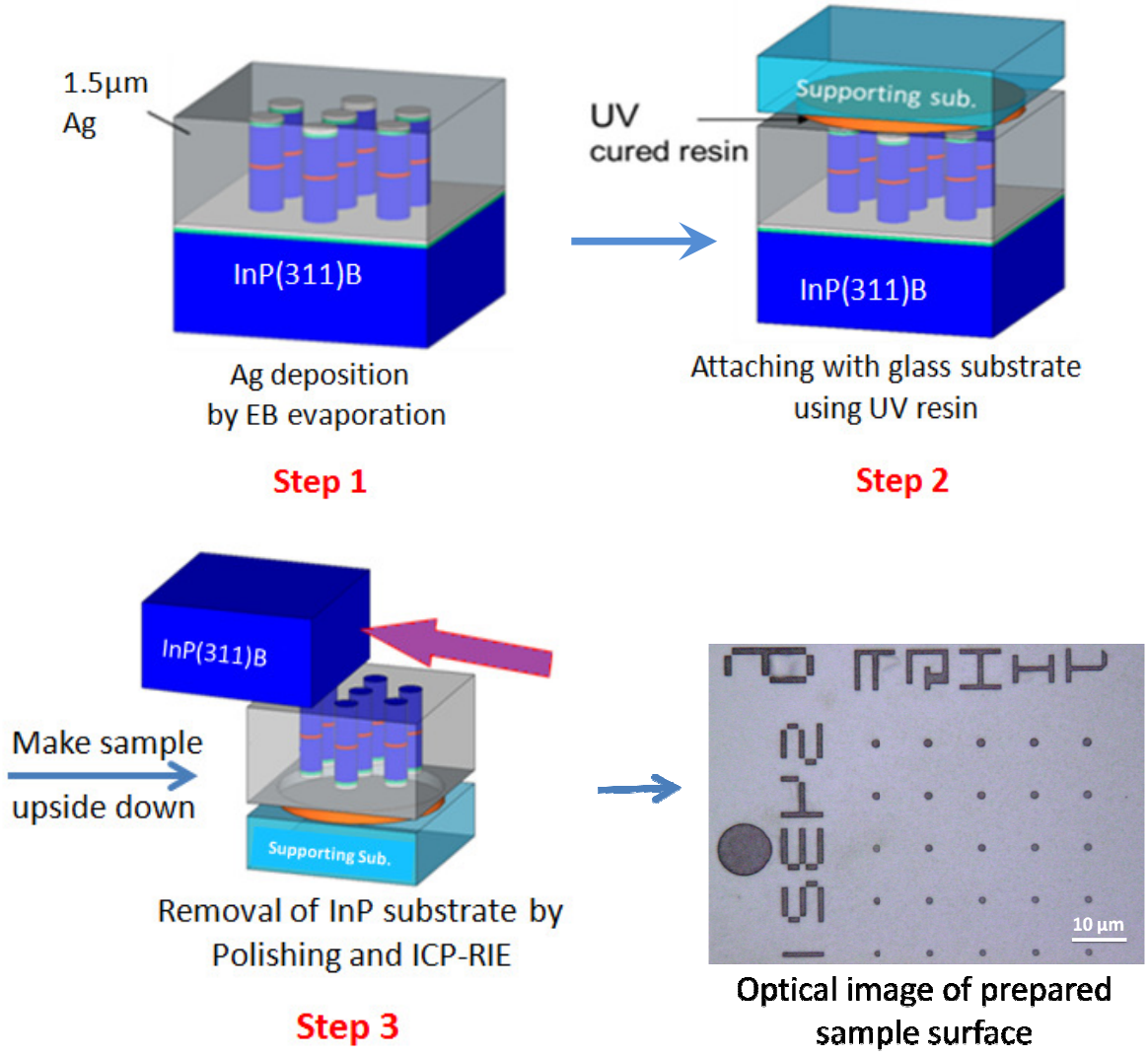

Fig. 3.5 Substrate removal procedure to obtain Ag embedded pillars for higher photon extraction efficiency.

Silver (Ag) was chosen as the embedding metal since Ag exhibits high optical reflectivity in the infrared spectral range and enhances extraction of emitted photons by the lateral reflection at the pillar-sidewall and Ag interface [8].

Figure 3.5 schematically shows the steps of fabricating Ag-embedded pillars to improve the photon extraction efficiency. After the deposition of Nb on top of the as-etched pillars, additional 1.5 µm thick silver (Ag) layer was evaporated to bury the pillars by e-beam evaporation method. Then, the sample was turned upside down and the Ag surface of the sample was pasted to a supporting glass substrate (microscope slide) using ultra violet (UV) curing resin, as shown in step 2 of Fig. 3.5.

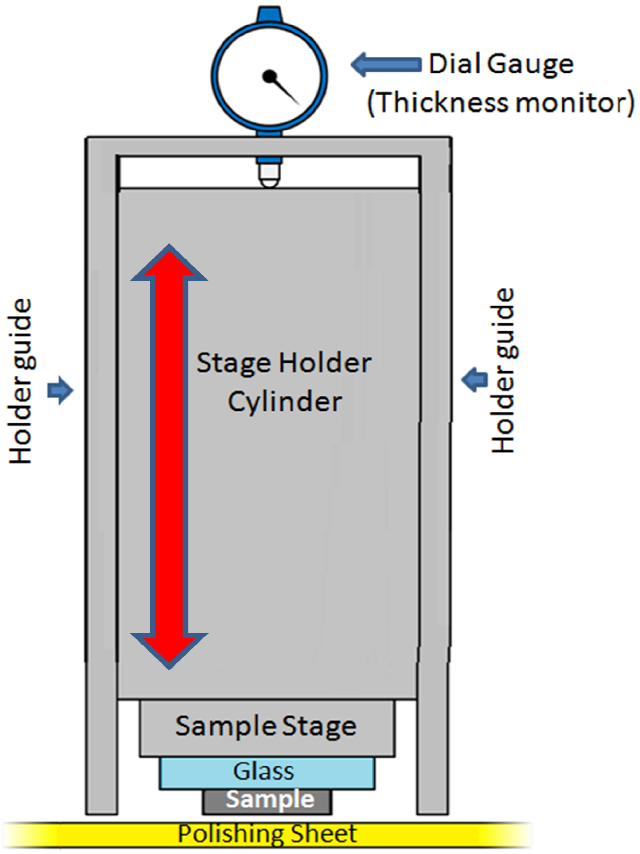

Fig. 3.6 Manual polishing machine used for polishing the InP substrate.

Finally, the InP substrate was removed with mechanical polishing and subsequent ICP-RIE. Figure 3.6 shows the manual polishing machine that was used for thinning the InP substrate before finalizing the process with ICP RIE. Several polishing sheets for mirror polishing, ranging from the particle size of 30 μm to 0.3 μm, were used for obtaining finely smooth surface of the substrate. For the final step of polishing, baikalox alumina polishing powder (0.3 μm particle size) was used.

After yielding a mirror-looking smoothly polished surface, ICP-RIE was performed to remove the remaining InP, so that the etching stops near the InP/Ag interface. This completes the fabrication process of the Ag-embedded pillars, and the sample is ready for the optical measurements. The bottom right image in Fig. 3.5 shows the top view optical image of the fabricated Ag-embedded pillars.

3.5 Band Structure of The Prepared Sample

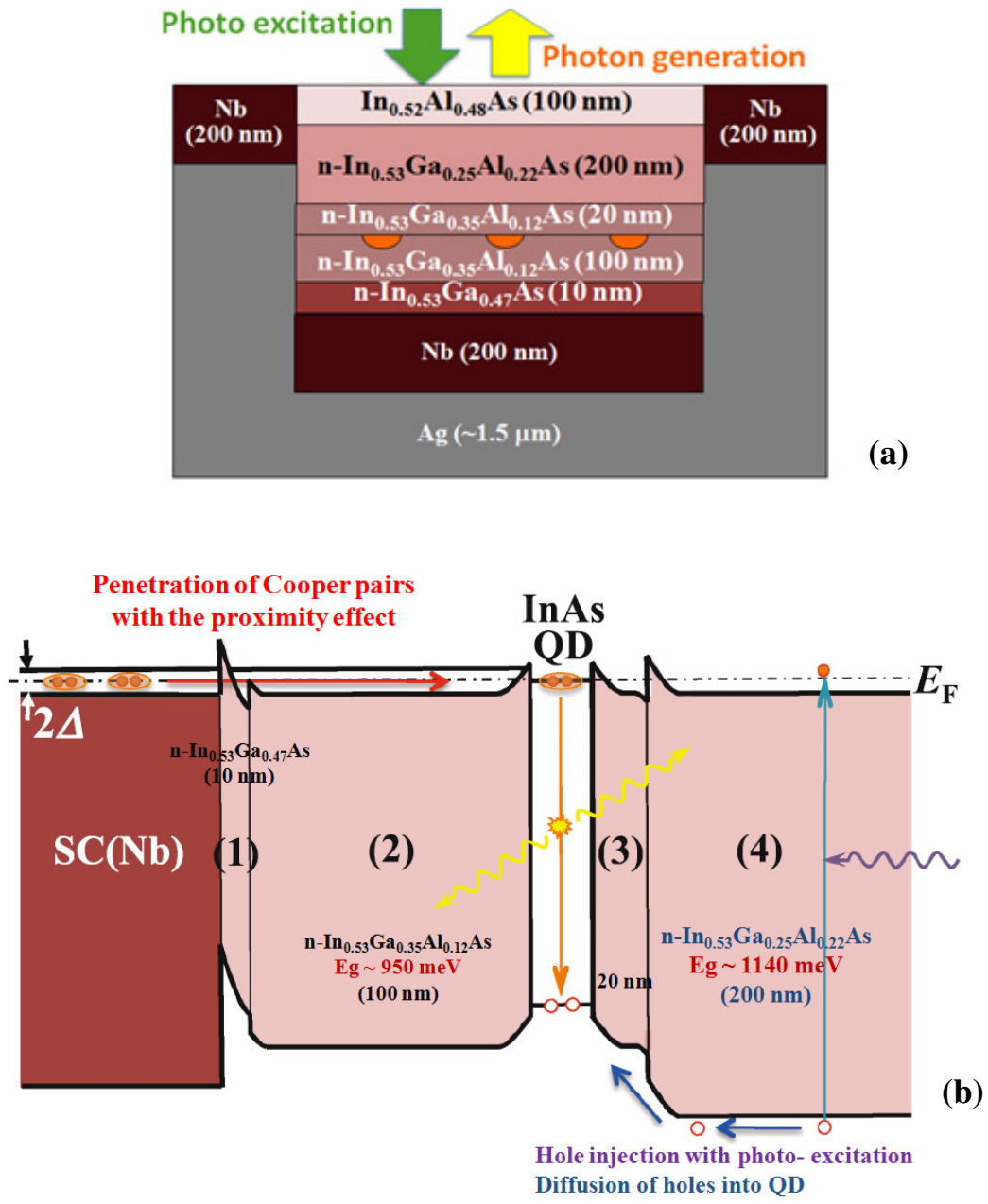

Fig. 3.7 **(a)** Schematic of Ag-embedded InAs QD heterostructure sample and **(b)** Schematic band structure of the sample.

Figure 3.7(a) shows the schematic of the prepared Ag embedded heterostructure with the detail specifications of the layers. The band diagram of the sample is shown in Fig. 3.7(b). The energy gap of $In_{0.53}Ga_{0.47}As$, $In_{0.53}Ga_{0.35}Al_{0.12}As$, and $In_{0.53}Ga_{0.25}Al_{0.22}As$ at low temperature is estimated to be 820, 950, and 1140 meV, respectively [9]. Electrons in Nb form spin-singlet Cooper pairs at a temperature below T_C. From Fig. 3.7(b) the Schottky barrier at the Nb/$In_{0.53}Ga_{0.47}As$ interface may be considered to prevent the penetration of electron Cooper pairs from the Nb superconductor to the semiconductor heterostructure. But the practical case can be properly understood by the following estimations.

The Schottky barrier height is estimated to be 196 meV [10]. The potential barrier will be further reduced by 51 meV with the Schottky effect [11]. Then, with the electron concentration of 1×10^{18} cm^{-3}, the depletion layer width is calculated to be 14.4 nm for a thick enough $In_{0.53}Ga_{0.47}As$ layer. However, due to the modulation doping from the adjacent $In_{0.53}Ga_{0.35}Al_{0.12}As$ barrier in Fig. 3.7(b), the electron concentration in the $In_{0.53}Ga_{0.47}As$ layer is higher and this makes the depletion layer width thinner than the $In_{0.53}Ga_{0.47}As$ layer thickness of 10 nm.

The proximity effect, that is, the penetration of electron Cooper pairs to a normal region depends on the coherence length of electron Cooper pairs, and it is calculated to be $9.16\times10^{-4}(N_{3D})^{1/3}/T^{1/2}$ [nm] from the known formula [12] and with the physical parameters for InGaAs [3]. N_{3D} is the electron concentration in the normal region (in this case, InGaAs), and for $N_{3D} = 1\times10^{18}$ cm^{-3}, the coherence length is $916/T^{1/2}$ [nm] at temperature T [K]. N_{3D} will be lower in the above-discussed depletion layer with the thickness of ~10 nm at the Schottky interface. In this thin depletion layer with the relatively low barrier height, electron wave function penetrates into the depletion layer, and this results in the effective residual electron concentration. Even if the electron concentration was three orders of magnitude lower, that is, 1×10^{15} cm^{-3}, the coherence length is estimated to be $91.6/T^{1/2}$ [nm], which is much longer than the depletion layer width at the Nb/$In_{0.53}Ga_{0.47}As$ interface. Thus, the penetration of electron Cooper pairs into the InGaAs-based heterostructure becomes possible.

With the modulation doping of the InAs QDs, the depletion layers appear in the $In_{0.53}Ga_{0.35}Al_{0.12}As$ barriers adjacent to the QDs. When the band offset of $\Delta E_C : \Delta E_V = 0.7:0.3$ is assumed in the InGaAs-based heterostructure [9], the conduction-band effective potential barrier height at the $In_{0.53}Ga_{0.35}Al_{0.12}As$/InAs QD interface can be calculated to be 112 meV. With the n-type doping of 1×10^{18} cm^{-3} in the $In_{0.53}Ga_{0.35}Al_{0.12}As$ barrier, the depletion layer width is estimated to be 12.7 nm. With the consideration similar to the above Schottky barrier tunneling, it is possible for Cooper pairs to tunnel the low-height barrier coherently through the InAs QDs.

3.6 Reports on Observation of Proximity Effect

Proximity effect is a term used in the field of superconductivity to describe the phenomena that occur when a superconductor (SC) is placed in contact with a non-superconductor, e.g. a normal metal. Below the critical temperature (T_C) of the superconductor, the normal metal in close proximity to the superconductor acquires SC properties, and the local density of states (DOS) of the normal metal is modified by the penetration of electron Cooper pairs. This phenomenon is known as the proximity effect.

Proximity effect has been studied for decades [13]. In 2013, L. Serrier-Garcia et al. revealed the proximity effect between a superconductor and a normal metal in their scanning tunneling spectroscopy (STS) experiment [14]. The normal metal surface that includes several SC islands was studied with STS, and the proximity effect, especially spatial extension of the SC properties from the superconductor interface to the normal metal surface, was directly observed. Opening of the SC gap and the modified SC DOS were observed on the normal-metal surface adjacent to the SC-island interface. Figure 3.8 schematically shows the STS experiment done by L. Serrier-Garcia et al. Figure 3.8(a) shows the STM image of the Pb islands interconnected by Pb wetting layer on undoped Si substrate and Fig. 3.8(b) explains

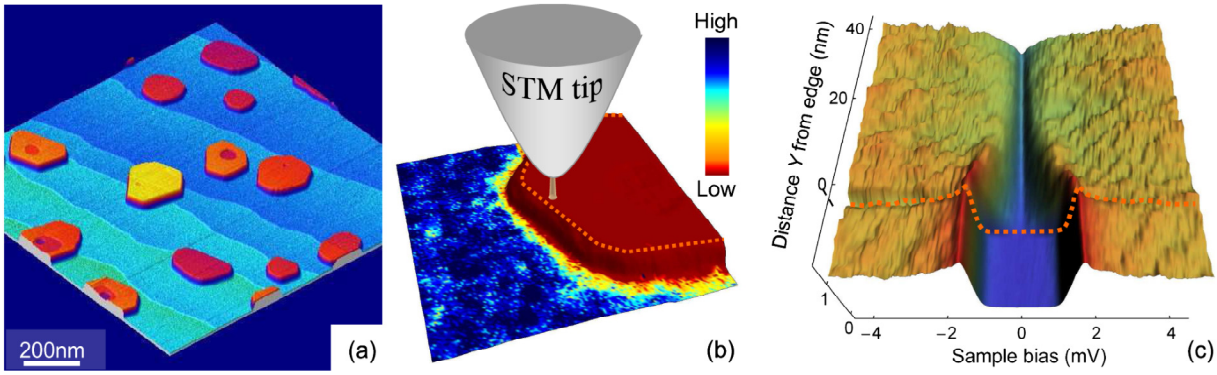

Fig. 3.8 (a) STM image of Pb superconductor islands in wetting layer on undoped Si substrate. (b) Color-coded STS tunneling conductance map superimposed onto 3D topographic STM image. The colors correspond to the conductance variations. (c) Spatial variations of the local dI(V)/dV spectra as a function of the distance from the island edge. The dashed line corresponds to the spectrum taken at the island edge [14].

the experimental geometry. Figure 3.8(c) yields the dependence of the SC properties in the normal region on the distance from the SC island edge, and the superconducting state in the islands is characterized by a fully opened gap shown by the dashed line in the bottom of this figure. In the wetting-layer-side region, far from the islands, the tunneling spectra exhibit a V-shaped dip at zero bias [upper curve in Fig. 3.8(c)]. As the STM tip proceeds to the island edge, the tunneling spectra evolve gradually from the non-superconducting to the superconducting gap shape thus evidencing the proximity effect.

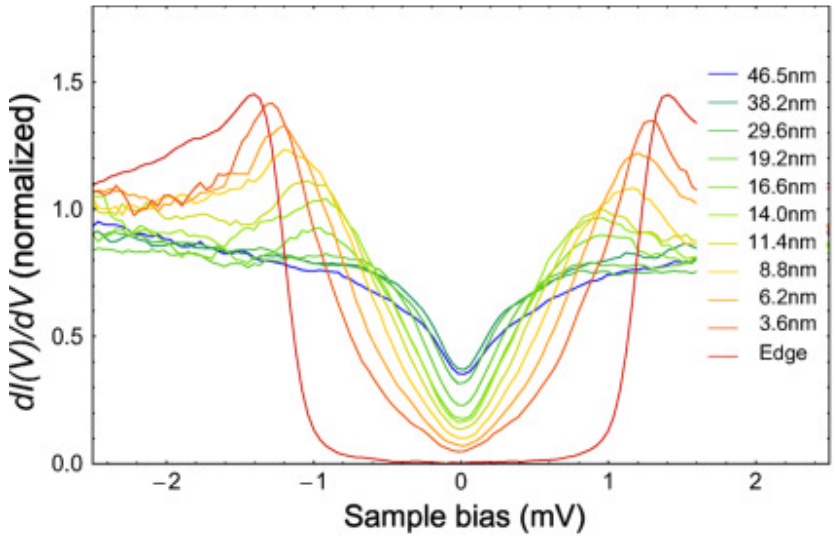

Fig. 3.9 Development of measured local tunneling conductance spectra (normalized) as a function of the distance from the island edge [14].

Figure 3.9 shows the change of measured local tunneling conductance spectra as a function of the distance from the island edge. At the edge, the tunneling spectra show the opening of SC gap. On moving far away from the edge the spectra evolve, on a scale of several nanometers, from a superconducting bulk like behavior to the V-shaped zero-bias anomaly.

Also, opening of the SC gap and the SC DOS induced in a semiconductor by the proximity effect was observed with InAs-aluminum (Al) semiconductor-superconductor nanowires with tunneling spectroscopy by W. Chang et al. [15], as shown in Fig. 3.10. Schematic cross

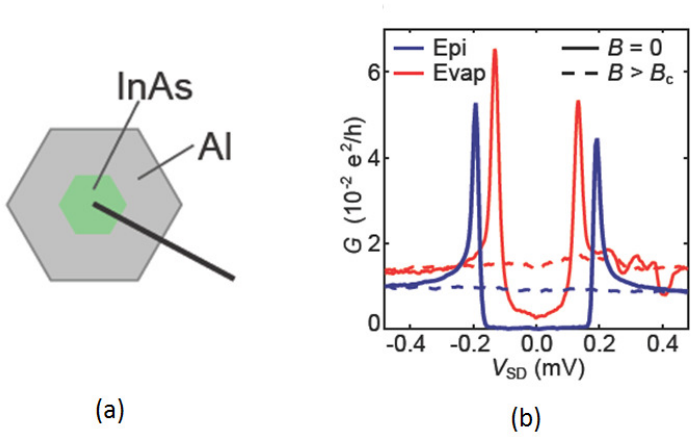

Fig. 3.10 (a) Schematic cross section of epitaxial full-shell nanowire with InAs core and Al shell and **(b)** Differential conductance as a function of source-drain voltage of an epitaxial full-shell device and an evaporated control device [15].

section of InAs-core and Al-shell nanowire is shown in Fig. 3.10(a) and the tunneling spectra of the experimental nanowire and an evaporated control device are shown in Fig. 3.10(b). In the superconducting state (when external magnetic field, B = 0), conductance (G) of the nanowire, as a function of source-drain voltage (V_{SD}), showed strongly suppressed conductance between symmetric peaks and a clear opening of SC gap is visible, while above a critical value of B both devices showed featureless normal-state tunneling conductance [15].

References:

[1] I. Suemune, T. Akazaki, K. Tanaka, M. Jo, K. Uesugi, M. Endo, H. Kumano, E. Hanamura, H. Takayanagi, M. Yamanishi, and H. Kan, Jpn. J. Appl. Phys., 45, 9264 (2006)

[2] Y. Hayashi, K. Tanaka, T. Akazaki, M. Jo, H. Kumano, and I. Suemune, Appl. Phys. Express 1, 011701 (2008)

[3] H. Sasakura, S. Kuramitsu, Y. Hayashi, K. Tanaka, T. Akazaki, E. Hanamura, R. Inoue, H. Takayanagi, Y. Asano, C. Hermannstaedter, H. Kumano, and I. Suemune, Phys. Rev. Lett. 107, 157403 (2011)

[4] N. A. Jahan, C. Hermannstaedter, J-H. Huh, H. Sasakura, T. J. Rotter, P. Ahirwar, G. Balakrishnan, K. Akahane, M. Sasaki, H. Kumano, and I. Suemune, J. Appl. Phys. 113, 033506 (2013)

[5] K. Akahane and N. Yamamoto, J. Cryst. Growth 378, 450 (2013)

[6] I. Suemune, H. Nakajima, X. Liu, S. Odashima, T. Asano, H. Iijima, J.-H. Huh, Y. Idutsu, H. Sasakura, and H. Kumano, Nanotechnology 24, 455205 (2013)

[7] H. Kumano, H. Nakajima, S. Ekuni, Y. Idutsu, H. Sasakura, and I. Suemune, Adv. Math. Phys. 2010, 1 (2010)

[8] H. Kumano, H. Nakajima, H. Iijima, S. Odashima, Y. Matsuo, K. Ijiro, and I. Suemune, Appl. Phys. Express 6, 062801 (2013)

[9] I. Vurgaftman, J. R. Meyer, and L. R. Ram-Mohan, J. Appl. Phys. 89, 5815 (2001)

[10] K. Kajiyama, Y. Mizushima, and S. Sakata, Appl. Phys. Lett. 23, 458 (1973)

[11] S. M. Sze, Physics of Semiconductor Devices, 2nd ed. (Wiley, New York, 1981)

[12] T. Akazaki, T. Kawakami, and J. Nitta, Appl. Phys. Lett. 66, 6121 (1989)

[13] P. G. de Gennes, Rev. Mod. Phys. 36, 225 (1964)

[14] L. Serrier-Garcia, J. C. Cuevas, T. Cren, C. Brun, V. Cherkez, F. Debontridder, D. Fokin, F. S. Bergeret, and D. Roditchev, Phys. Rev. Lett. 110, 157003 (2013)

[15] W. Chang, S. M. Albrecht, T. S. Jespersen, F. Kuemmeth, P. Krogstrup, J. Nyg°ard, and C. M. Marcus, Nat. Nanotechnol. 10, 232 (2015)

Chapter 4

Cooper Pairs Recombination in InAs Quantum Dots: CW Measurements

Photoluminescence (PL) is defined as the spontaneous emission of light from a material under optical excitation and can be therefore used to provide detailed information on electronic states involving both intrinsic and extrinsic optical processes of that material. PL spectroscopy is a non-contact method of probing the electronic structure of materials. PL spectroscopy of semiconductors is popularly done by directing light, typically from a laser with its energy higher than the fundamental band gap of the semiconductor, onto the semiconductor sample where light is absorbed and photo-excitation occurs. This causes the excited electrons to jump to the conduction band leaving the holes in the valence band and thus generating electron-hole pairs. The photons emitted upon recombination of the electron-hole pairs correspond to the energy difference between the valence and conduction bands.

To study the optical properties of the prepared Ag-embedded Nb-superconductor/InAs QDs based n-InGaAs heterostructure, PL was observed by the optical access from the backside of the sample through the InP substrate. Continuous wave (CW) luminescence measurements were performed on the sample, above and below the superconducting critical temperature (SC T_C) of the deposited Nb superconductor, to analyze the Cooper pairs effect on the luminescence of the InAs QDs.

In this chapter, the details of CW PL spectroscopy of the prepared sample and the obtained results are discussed. CW PL spectroscopy is the commonly performed optical spectroscopy in which photon emission is recorded or accumulated for a desired period of time with the application of CW laser excitation of the sample.

4.1 Experimental Setup and Measurement Method

For CW PL measurements, the prepared sample was placed in a liquid-helium cooled cryostat and its temperature was lowered and maintained between 4 K to 12 K. The sample was excited with CW helium – neon (He – Ne) laser operating at ~633 nm and the laser spot diameter on the sample was ~ 2 µm. The laser was focused onto one Ag embedded nanopillar at a time with an objective lens (OL) of 0.4 numerical aperture (NA) to observe the PL of that selected pillar. PL of QDs was collected with the same objective lens and was dispersed by a 50-cm double monochromator with 300-grooves per-mm gratings and was finally detected with a liquid-nitrogen-cooled InGaAs-photodiode array detector. The temperature of the sample was varied from 4 K to 12 K during a measurement by controlling the flow of liquid He in the cryostat and heating. Figure 4.1 shows the experimental setup used for the CW photoluminescence measurement.

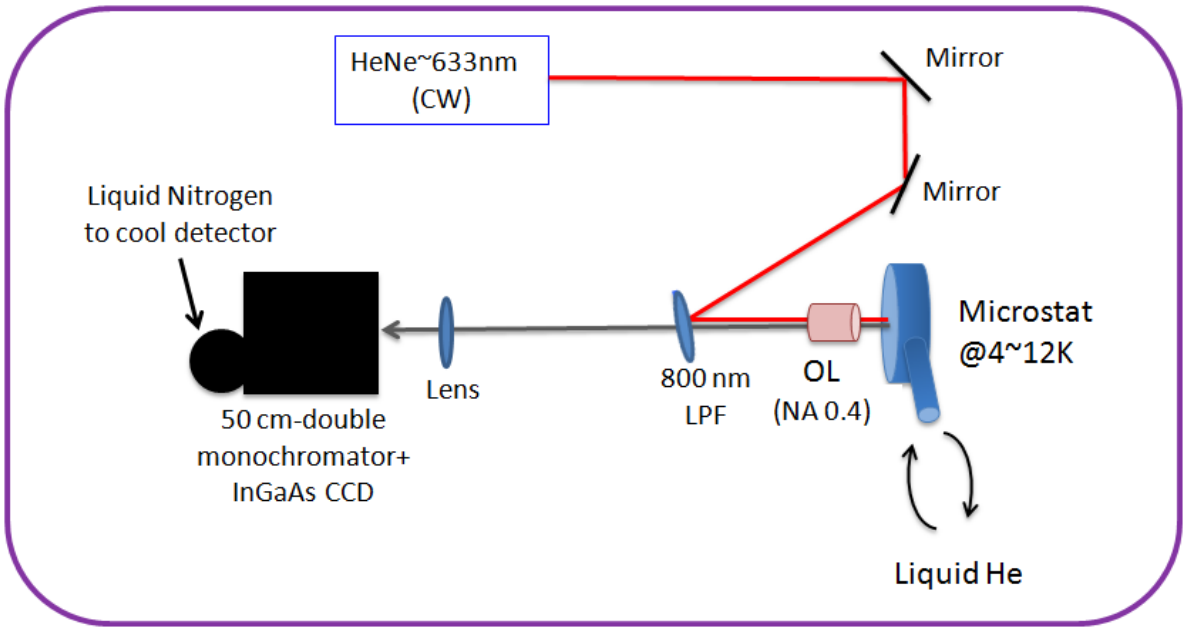

Fig. 4.1 Experimental setup for photoluminescence spectroscopy with CW laser.

4.2 Cooper Pairs Luminescence from InAs QDs

Figure 4.2 shows the PL spectra of the prepared Ag-embedded Nb-superconductor/InAs QDs based n-InGaAs heterostructure sample measured on one of the pillars with the diameter of 1.5 µm. The power of the He – Ne exciting laser was 20 µW. The focused beam diameter is estimated to be 2 µm, and almost the whole pillar surface was covered by the laser beam. This gives the excitation power density of 600 W/cm^2. With the given QD density of

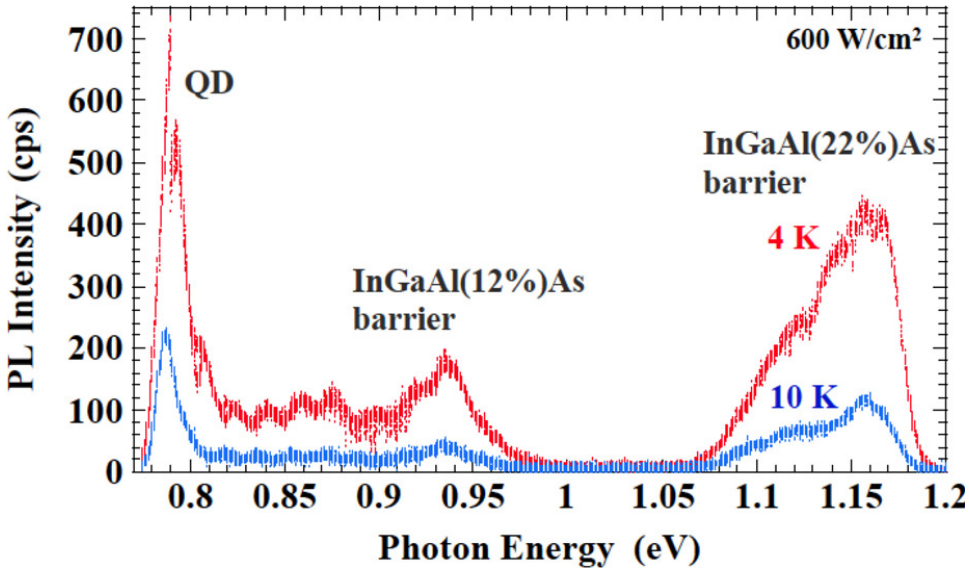

Fig. 4.2 Photoluminescence spectra of the prepared sample measured on one of the pillars with diameter 1.5 µm, below and above SC T_C of Nb (~ 9.09 K).

3.4×10^{10} cm^{-2}, as mentioned in the previous chapter's section 3.1, this pillar includes about ~ 600 QDs. Under the mentioned excitation power density (600 W/cm^2), the PL spectra were measured at 4 K and 12 K, which are below and above the SC T_C of Nb (~ 9.09 K), respectively. As we can see in Fig. 4.2, three major peaks are observed in the PL spectra around 790, 950, and 1150 meV, and are identified as the luminescence originated from the InAs QDs, $In_{0.53}Ga_{0.35}Al_{0.12}As$, and $In_{0.53}Ga_{0.25}Al_{0.22}As$ barriers, respectively. The QD PL intensity measured at 4 K is almost three times larger than that measured at 12 K. This huge enhancement of PL intensity below the SC T_C clearly suggests the superconducting effect on the luminescence of the heterostructure.

It is also observed from Fig. 4.2 that the PL enhancement below SC T_C happened for all the three peaks, that is, the InAs QD emission as well as the barriers emission. The explanation of this behavior is possible from the energy band structure of the sample (Fig. 3.7(b)). The conduction-band edges in all the semiconductor layers through the whole heterostructure are aligned to the common Fermi level with the relatively high n–type doping of $\sim 1 \times 10^{18}$ cm^{-3}. The potential barriers at the heterointerfaces are estimated to be relatively low values of 90 – 130 meV [1] and the related depletion layer widths are on the order of 10 nm. Since the Cooper-pair coherence length in the n-type semiconductors is estimated to be ~1300 nm at 1 K, ~650 nm at 4 K, and ~450 nm at 8 K [2, 3], it is possible for electron Cooper pairs to penetrate from the Nb superconductor into all the n-type doped layers. Under this situation, photon emission is rate-limited by the counterpart hole injection in the valence band with the absorption of the exciting laser light. The absorption is dominated by the surface $In_{0.53}Ga_{0.25}Al_{0.22}As$ barrier layer, but the subsequent hole diffusion into the inner InAs QDs and the $In_{0.53}Ga_{0.35}Al_{0.12}As$ barrier layers also generates photons from these layers, as observed in Fig. 4.2. Therefore the drastic luminescence enhancement at the lower temperature of 4 K is attributed to the penetration of the electron Cooper pairs deep into the heterostructure up to $In_{0.53}Ga_{0.25}Al_{0.22}As$ barrier layer through InAs QDs and the inner $In_{0.53}Ga_{0.35}Al_{0.12}As$ barriers [4].

Figure 4.3(a) shows the temperature dependence of InAs-QD luminescence spectra measured on another pillar with a diameter of 1.5 μm [5]. The excitation laser power density was $600 W/cm^2$. Although the temperature-dependent variation of the luminescence spectra is modest, the peak intensity shows drastic change near T_C of Nb. The temperature dependence of the QD luminescence peak intensity is shown in Fig. 4.3(b) and an abrupt increase of the peak PL intensity is clearly observed at T_C of the Nb superconductor. This reproduces the luminescence intensity enhancement previously observed in SC LEDs, mentioned in section 2.4 of Chapter 2 [6, 7]. This clear correlation to T_C demonstrates that the phenomenon is closely related to superconductivity.

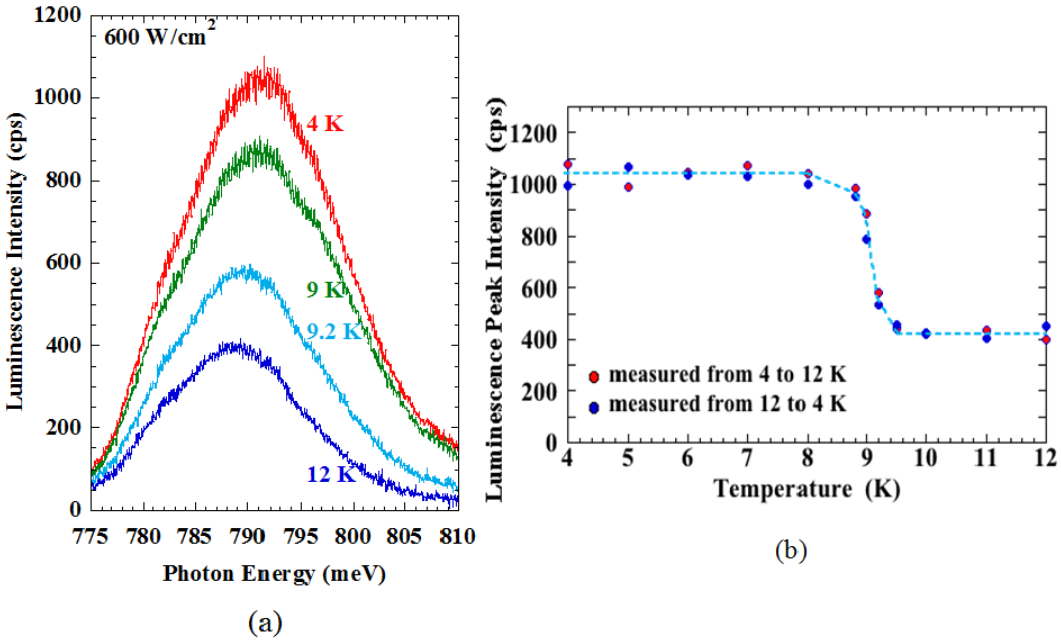

Fig. 4.3 (a) Temperature dependence of InAs-QD luminescence spectra and (b) Temperature dependence of QD luminescence peak intensity. To confirm the relation to T_C of Nb ~ 9.09 K, measured data for the temperature rising and falling sequences are shown.

It is observed from Fig. 4.3(a) that the luminescence peak is around 790 meV and is slightly blue-shifted for the lower temperature. This can be interpreted with the schematic shown in Fig. 4.4, where the distribution of QD sizes and therefore of the QD discrete energy states are symbolically represented with a larger QD and a smaller QD. The conduction band of the QD states are modulation-doped from the adjacent heavily n-type doped barrier layers, and the QD states in the conduction band share the same Fermi level as the barrier layers. The QD luminescence is regulated by the minority holes in the QD ground state in the valence band injected by the diffusion from the photo-excited barrier layers. At temperature above the SC T_C (12K in Fig. 4.3(a)), the PL peak is observed at slightly lower energy than 790 meV. This is symbolically represented with the luminescence from the larger QD in Fig. 4.4. At the temperature much lower than the SC T_C, the SC gap opens near the Fermi level in the conduction band by the proximity effect and photon emission from the smaller QDs, where their conduction-band QD states are nearly in resonance with the superconducting density of states (SC DOS), is enhanced because of the energy-condensed SC DOS. This shifts the

apparent PL peak toward the higher photon energy and causes the blueshift. The BCS SC DOS shown in Fig. 4.4 has been calculated with the well-known formula [8].

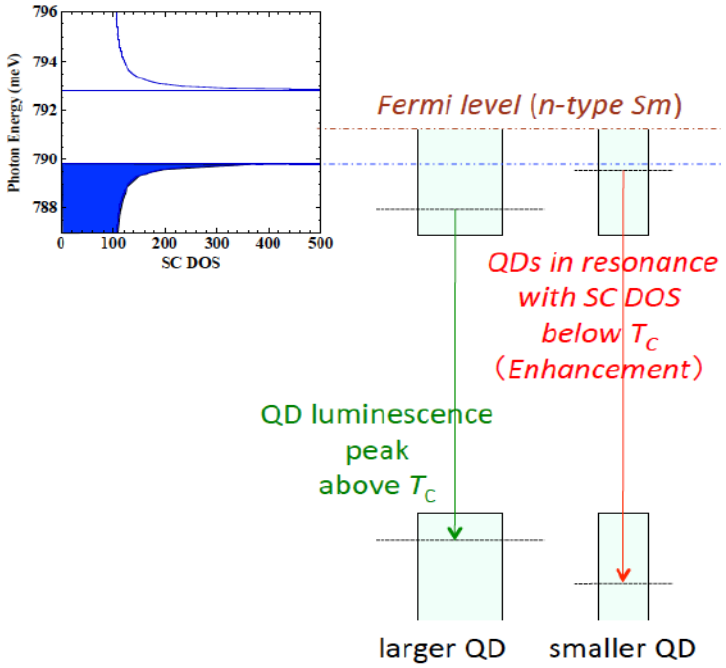

Fig. 4.4 Schematic to show the relation between the SC DOS induced by the proximity effect and the luminescence of QDs. The energy-condensed DOS enhances the luminescence from the smaller QDs, of which conduction-band energy state is near in resonance with the SC DOS.

4.3 Signature of SC-DOS in InAs-QD Luminescence Spectra

I have worked on similar luminescence measurements on the InAs QD emission of the same pillar, with a diameter of 1.5 µm, whose PL spectra is shown in Fig. 4.2 and I observed a sharp edge in the QD luminescence spectra. In this section, I will discuss about this special feature observed in the QD PL spectra.

4.3.1 Appearance of Sharp Edge in the QD Luminescence Spectra

The results of the PL measurements performed on another pillar with the diameter of 1.5 µm are shown in Fig. 4.5. The spectra were measured at temperatures below and above SC T_C of deposited Nb (~ 9.09 K). Figures 4.5(a) and 4.5(b) show the PL spectra measured with strong (600 W/cm^2) and weak (30 W/cm^2) excitation power densities, respectively. It is observed that the luminescence intensity is highly enhanced at 4 K in comparison to higher temperatures above SC T_C, 10 K in Fig. 4.5(a) and 9.1 K in Fig. 4.5(b). This correlation of the luminescence intensity to SC T_C reproduces that of Fig. 4.3.

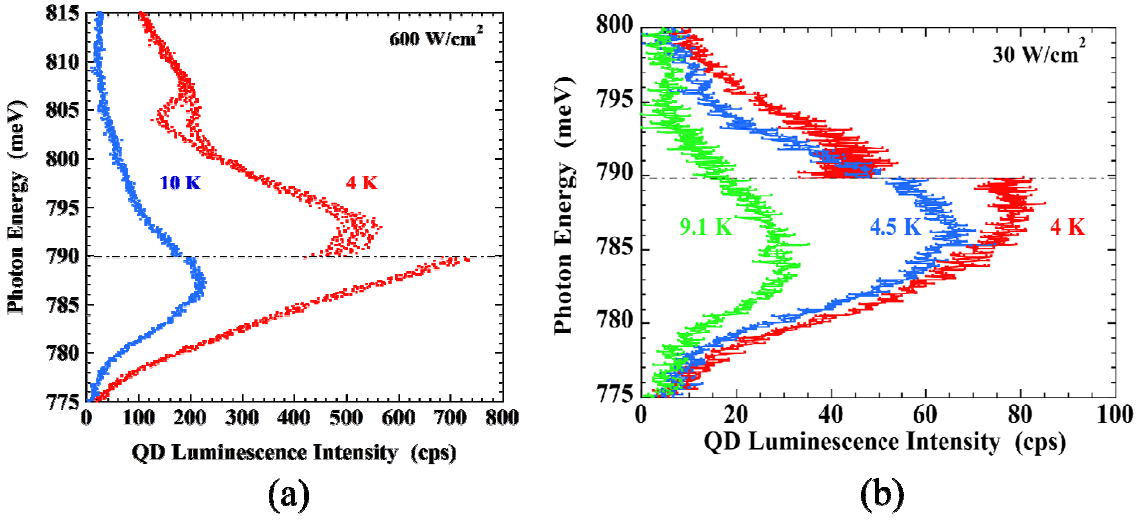

Fig. 4.5 Luminescence spectra of InAs QDs observed from another pillar with the diameter of 1.5µm at temperatures below and above SC T_C (~ 9.09 K), (a) with strong (600 W/cm^2) and (b) with weak (30 W/cm^2) excitation power. The alternate long and short dashed black line in both figures is the guide to the eye, indicating the luminescence intensity sharp edge.

The distinct feature of Fig. 4.5(a) is that a sharp peak and a sharp edge are observed at the photon energy of ~790 meV below T_C. The sharp edge disappears above T_C. This same sharp feature is also observed in Fig. 4.5(b), for the PL spectra measured at 4 K with the weaker photo excitation. From Fig. 4.5(b), it is found that this special sharp feature is very sensitive and easily disappears with a slight temperature rise when the photo excitation is weak. Luminescence intensity instability is also observed from Fig. 4.5(a), in the photon energy range of 790 – 793 meV and 801 – 806 meV below T_C. These unusual features observed in the InAs-QD luminescence spectra below T_C manifest the superconductivity effect in the luminescence processes of QDs. I have studied modeling of the observed phenomena considering the superconductivity effect in radiative recombination processes of QDs in the following sub-section and discussed the relation of the luminescence intensity enhancement and the distinct spectral change below T_C.

4.3.2 Model Fitting of Observed Luminescence Spectra

As I have already discussed in Section 3.6 of Chapter 3, the opening of SC gap on a normal region surface which is in close proximity to a superconductor by the proximity effect was directly observed with STS [9]. It was also observed that SC DOS is broadened with the increase of the distance from the superconductor/normal interface. This broadening was attributed to a finite-lifetime effect of quasiparticles at the SC gap edge state. This effect was included in the Bardeen-Cooper-Schrieffer (BCS) theory by adding an imaginary part to the quasiparticle energy E of the SC DOS [10],

$$N(E,\Gamma)/N_0 = Re\left[\frac{E_F - E + i\Gamma}{[(E_F - E + i\Gamma)^2 - \Delta^2]^{\frac{1}{2}}}\right] \qquad (4.1)$$

where E_F is the Fermi energy in the conduction band, Δ is the half of the SC gap and Γ is the phenomenologically introduced lifetime broadening. N_0 is the DOS in the normal state. Re[ ] is the real part of the physical quantity.

As mentioned earlier, the measured pillar had a diameter of 1.5μm and the number of QDs involved in the luminescence of such a pillar is estimated to be ~600. The conduction band

of the InAs QDs is modulation doped from the neighboring n-type $In_{0.53}Ga_{0.35}Al_{0.12}As$ barriers and is filled with electrons up to the Fermi energy, as schematically shown in the band structure in chapter 3 (Fig. 3.7(b)). Luminescence from the QDs is regulated by the hole population originated with the external photo excitation in the valence-band QD lowest-energy states. Considering the estimated large number of QDs, the energy distribution of the QD lowest-energy states that contribute to the photon emission is approximated with a Gaussian function as follows,

$$G(E) = N_{QD} \exp\left[-\frac{(E-E_F-\delta)^2}{\Delta E^2}\right] \qquad (4.2)$$

where E is the photon energy and $\sqrt{2}\Delta E$ is the half energy width of the Gaussian distribution. δ is the energy separation between the ensemble Gaussian peak energy and the Fermi energy E_F (Here E_F indicates the energy separation of conduction and valence band energy states of a QD whose conduction-band energy state is in resonance with the electron Fermi energy. In other words, the energy reference is the valence band state energy of that QD). N_{QD} is a constant proportional to the total number of luminescent InAs QDs. In general, radiative recombination rate is proportional to the density of states (DOS) of a relevant medium. Considering the modification of the local DOS with the superconductivity effect, the observed luminescence spectra can be fitted with the product of equations (4.1) and (4.2), i.e., $G(E)N(E,\Gamma)$. The details of the model fitting are described below with the excitation power dependent PL spectra.

The excitation power dependence of the QD luminescence spectra was measured at 4 K, where the minority hole population in the InAs QDs changes with the level of excitation. The measured luminescence spectra are shown in Fig. 4.6(a) for 75, 300, and 600 W/cm^2 and Fig. 4.6(b) for 30 and 150 W/cm^2. It is observed that the sharp edge at ~790 meV becomes sharper with the higher excitation, while it becomes less distinct for the lower excitation. The luminescence intensity instability in the photon-energy range of 790 – 793 meV is consistently observed, regardless of the excitation power. The instability in the photon-energy range of 801 – 806 meV is more distinct for the higher excitation power.

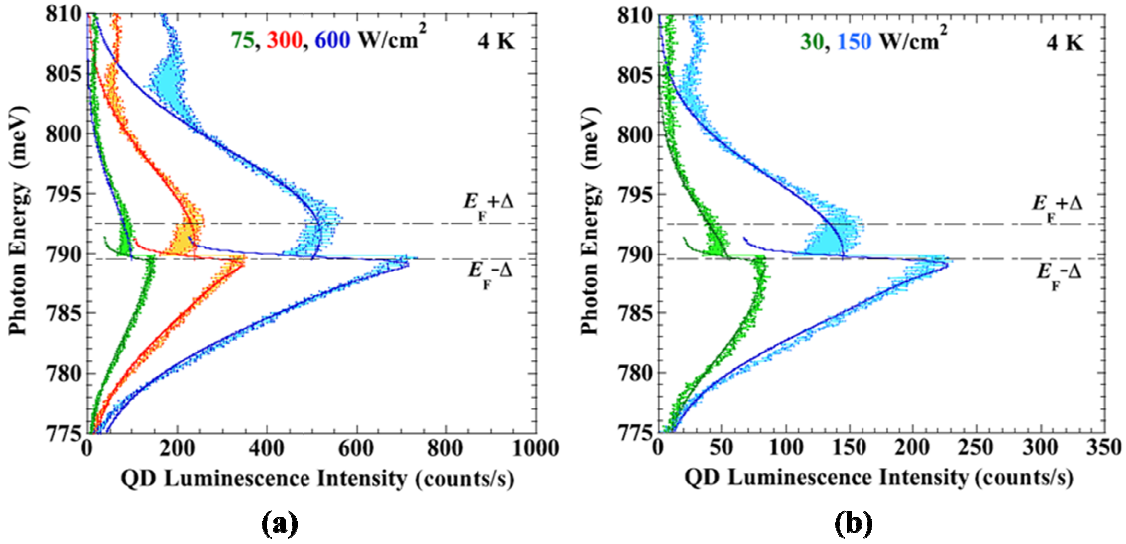

Fig. 4.6 Measured excitation power dependence of QD luminescence spectra. The measured photon counts are connected with neighboring counts with thin lines: (a) 75, 300, and 600 W/cm^2; (b) 30 and 150 W/cm^2. The solid lines are fitting with the parameters of E_F = 791.0 meV and Δ = 1.42 meV.

The solid lines in Fig. 4.6 are the model fitting with Eqs. (4.1) and (4.2). For this fitting, the electron Fermi energy was assumed to be E_F = 791.0 meV. The SC gap $2\Delta_0$ of Nb at 0 K is reported to be 2.91 ± 0.035 meV [11]. Based on the temperature dependence of the SC gap predicted by the BCS theory [10], a half of the SC gap Δ is estimated to be 1.42 meV at 4 K. The energy range within the alternate long and short dashed black lines corresponds to the SC gap. Regarding the empty SC DOS above the SC gap, it was assumed that there was no additional enhancement of the QD photon emission originating from the modified DOS. Therefore, the solid line for the energy above E_F + Δ is calculated with the QD Gaussian function of Eq. (4.2), and this line is tentatively extended into the SC gap region. The fitting with the product of Eqs. (4.1) and (4.2) was tentatively terminated at the middle of the SC gap by the consideration of the SC DOS lifetime broadening.

The situation is more complex within the SC gap considering the Cooper-pair tunneling process to each QD state. Cooper-pair's transport through a QD state depends on whether a single electron is present or not in the QD state beforehand due to strong Coulomb interactions [12]. Supercurrent carried by Cooper pairs is reversed coherently if a single electron is present in the QD state, and then coherent interference of supercurrent takes place. Population of QD states near the Fermi level varies with time during the luminescent event with the external photoexcitation, and therefore coherent interference of supercurrent is time dependent. The luminescence intensity instability observed in the SC gap reflects this time-varying supercurrent flow to the conduction-band QD states of the InAs QDs. The QD luminescence above the photon energy of ~804 meV originates from the QD excited states. The population instability in the lowest-energy QD states, especially that of minority holes, influences the population of the excited states. Hence, the luminescence intensity instability observed around the photon energy of 804 meV is related to the induced population instability in the first excited states. Since the population of the excited states increases for the higher photoexcitation, the instability around the photon energy of 804 meV is more distinct for the higher excitation power in Fig. 4.6.

The SC DOS with the lifetime broadening used for the fitting of the QD luminescence spectra is shown in Fig. 4.7. The value of the lifetime broadening Γ, used for the fitting of all the spectra shown in Fig. 4.6, is 0.6 meV. The SC DOS without broadening (Γ = 0 meV) is also shown as a reference. The Gaussian distribution of the QD energy states, shown in Fig. 4.7, is the one used for the fitting of the spectrum above the SC DOS observed with the photoexcitation power of 600 W/cm^2 in Fig. 4.6(a). The peak energy of the Gaussian distribution is shifted by δ from the Fermi energy E_F, and δ = 0.5 meV was used in Fig. 4.7.

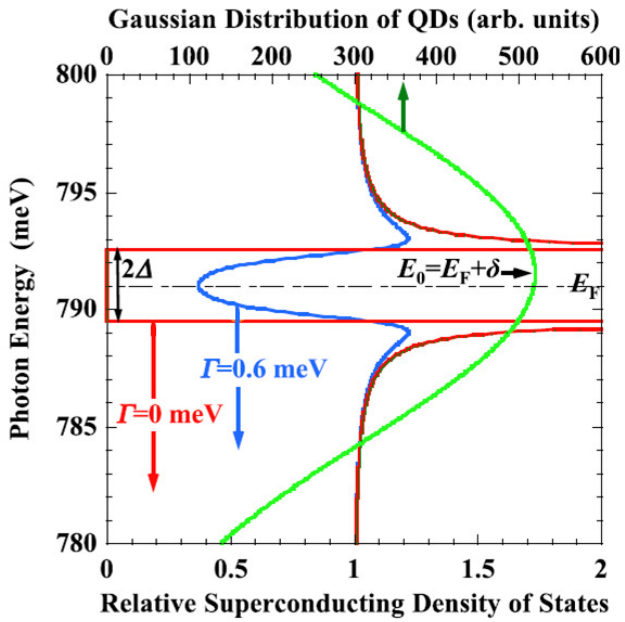

Fig. 4.7 Broadened SC DOS with Γ = 0.6 meV and Gaussian distribution of QD energy states employed for the fitting in Fig. 4.6 are shown. The Gaussian peak is given by $E_0 = E_F + \delta$, where E_F is the Fermi energy. In this figure, the energy separation of the Gaussian peak δ from E_F is given as 0.5 meV for the case of 600 W/cm^2 photoexcitation. SC DOS without broadening (Γ = 0 meV) is also shown. 2Δ is the SC gap.

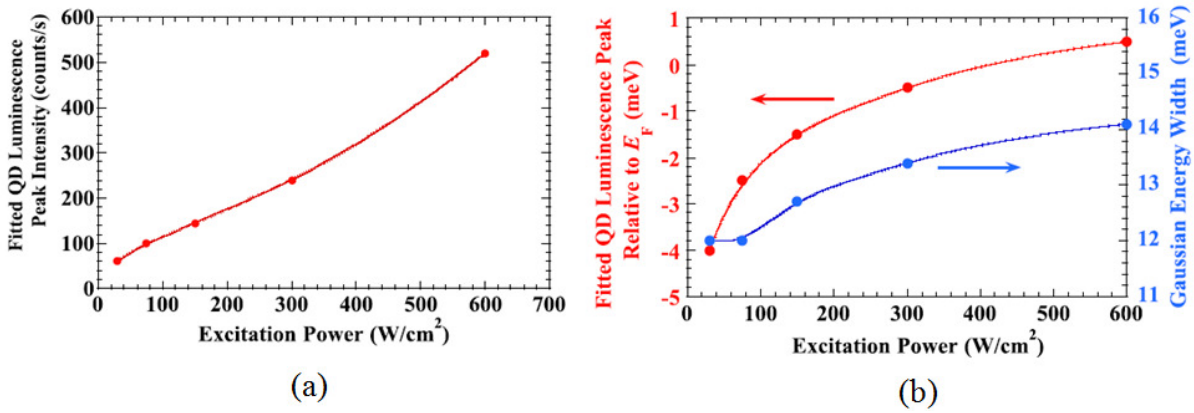

Fig. 4.8 Excitation power dependence of the Gaussian-function parameters used for fitting the spectra in Fig. 4. (a) The QD PL peak intensity. (b) The QD PL peak energy relative to the electron Fermi energy (given by the energy separation δ) and Gaussian half energy width (given by √2ΔE).

The excitation power dependence of the Gaussian function parameters used for the fitting of each spectrum is shown in Fig. 4.8. The fitted QD luminescence peak intensity, shown in Fig. 4.8(a), and the half energy width $\sqrt{2}\Delta E$ shown in Fig. 4.8(b) naturally increase for the higher excitation power. The fitted QD luminescence peak energy, shown in Fig. 4.8(b), given by the energy separation δ from the Fermi energy E_F, is blue-shifted for the higher excitation power due to the hole population filling in the valence-band QD states. This result clearly shows that the QD luminescence peak is energetically close to the SC gap for the higher excitation in the present sample, and the sharp edge is more clearly observed below T_C. On the other hand, the QD luminescence peak is red-shifted below the SC gap for the lower excitation, and the effect of the SC DOS on the luminescence spectra becomes milder.

4.4 Discussion

In the previous SC LEDs with QW active layers (discussed in Section 2.4 of Chapter 2), luminescence intensity enhancement [6, 7] and photon emission rate enhancement [2, 3] below T_C of the Nb SC electrodes were demonstrated, and the observed superconductivity effect was quantitatively well explained with the theory [13]. However, their luminescence spectra showed little variation below and above T_C. This is attributed to the continuous QW DOS.

The ensemble QD luminescence is generally fitted with the Gaussian function (random energy distribution of individually independent QD emission lines), but each single QD emission is intrinsically sharp discrete lines. A QD emission line width of ~50 μeV from an InAs QD with undoped InGaAlAs barriers, grown on an InP (311)B substrate in the similar manner as my experimental sample by molecular beam epitaxy (MBE), was observed by X. Liu et al. [14]. In my measurements, the enhancement of QD luminescence is modified, depending on whether QD energies are in resonance or off resonance to the SC DOS, and this produces the sharp edge in the QD luminescence spectra, reflecting the individual sharp QD emission lines. This sharp edge is averaged out in case of the continuous DOS in QW structures. However the situation changes when the superconductivity effect is assumed both in the conduction and valence bands [15], where the photon energy of the luminescence enhancement is definitely determined by the energy separation of the conduction-band and valence-bands SC DOS.

Another important difference between the QW- and QD-based systems is the energy distribution of photoexcited holes. In the case of QDs, excited holes are distributed among QDs, depending on their energy relaxation processes, and the Gaussian-broadened ensemble luminescence is generally observed. On the other hand, in doped QWs, schematically shown in Fig. 4.9, excited holes relax to the band edge of the lowest subband. The luminescence related to the Fermi level in the conduction band takes place with the valence-band state with the energy shifted by $(m_e/m_h)E_F$, where m_e and m_h are the electron and hole effective masses, respectively. Experimentally, the Fermi energy-related luminescence peak has been

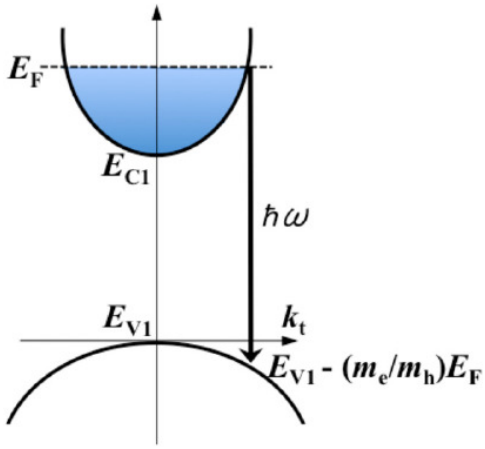

Fig. 4.9 Schematic band diagram of a doped QW. E_{C1} and E_{V1} are the lowest subband energies in the conduction and valence band, respectively. k_t is the wave vector in the QW plane. The arrow in the downward direction indicates the photon emission with the photon energy of ħω from the Fermi level to the valence band QW state.

observed with a modulation-doped 25 monolayer (ML) thick GaAs/AlGaAs QW at 2 K, and this peak was blue-shifted by 81.6 meV from the main luminescence peak [16]. Although the energy shift will be much less in the previously mentioned InGaAs QW-based SC LEDs with the lower barrier height [6], this experiment suggests that the possibility to observe the luminescence spectra related to the SC DOS near the Fermi level with the previous SC LEDs is less compared to the QD based SQLEDs.

Concerning the lifetime broadening of 0.6 meV used for fitting the QD luminescence spectra (Fig. 4.6(a) and 4.7), the broadening of SC DOS mainly takes place in the 100 nm thick $In_{0.53}Ga_{0.35}Al_{0.12}As$ barrier layer. For analyzing the broadening mechanisms, the influence of elastic impurity scattering and inelastic scattering, such as electron-phonon and repulsive electron-electron interactions on Cooper-pair luminescence was considered [13]. As I have mentioned in Chapter 1 that I also worked on time-resolved measurements of Cooper-pair luminescence from InAs QDs and measured the temperature dependence of the Cooper-pair

radiative recombination rate [17]. The details are discussed in the next chapter, but I could fit the measured Cooper-pair recombination rate enhancement below T_C employing the broadening parameter of $\Gamma \sim 1.2$ meV based on the above mentioned theory. This lifetime broadening may be sample dependent, but this value is reasonably close to the present fitted value of 0.6 meV.

Semiconductor QDs frequently exhibit spectral diffusion, that is, time-dependent reversible spectral shift of QD emission lines is observed [18]. This is attributed to the Stark effect caused by fluctuating local electric fields originating from charging and discharging of nearby impurities. Energy shifts up to 3.5 meV have been observed by J. Seufert et al. [18]. The spectral diffusion will quench the spectral resonance of QD emission lines to the SC DOS, and will change the tunneling processes of Cooper pairs to QD states time dependently and terminate the coherent transport of supercurrent through QD states. This possibly contributes to the effective additional lifetime broadening of SC DOS interacting with QD states.

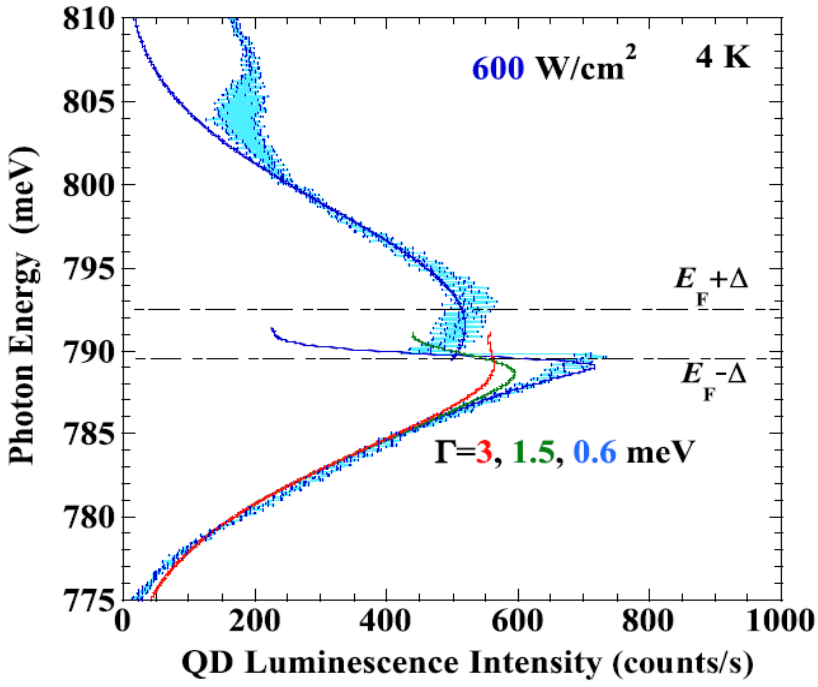

Fig. 4.10 Lifetime-broadening dependence of the fitted luminescence spectra for the one observed with the excitation power of 600 W/cm^2.

The comparison of the QD luminescence spectra, shown in Figs. 4.3(a) and 4.5(a), raises the question why the sharp edge is not always observed in the luminescence spectra from the InAs QDs in the same heterostructure sample. Actually, the lifetime broadening discussed above is dependent on the local environment around QDs and is dependent on samples. From this viewpoint, I have studied the lifetime broadening effect on the observed QD luminescence spectrum at the excitation power of 600 W/cm^2, and the result is shown in Fig. 4.10. It is observed that, with the increase of the broadening parameter Γ from 0.6 meV, the sharp edge in the luminescence spectrum is diminished. It is almost indistinguishable for Γ = 3 meV. Therefore, it can be concluded that cleaner environment around QDs, which reduces scattering of Cooper pairs and spectral diffusion of QD emission lines, is necessary for the observation of the signature of the SC DOS in the QD luminescence spectra.

The analysis that considers effects of Cooper pairing on the recombination process [13] explains the enhancement of luminescence intensity below T_C. According to the BCS theory, effects of SC correlation would be energetically limited within an energy range of $E_F \pm \Delta$. On the other hand, the luminescence intensity experimentally measured in Figs. 4.3(a) and 4.5(a) is enhanced in the wider energy range than $E_F \pm \Delta$ at low temperature. As discussed above on my experimental results, there are several factors that may broaden the effective energy range. I have considered a broadening effect due to the distribution in energy levels among QDs through Eq. (4.2) for fitting the data in Fig. 4.6 and 4.10. Such a broadening effect, however, could be explained in more convincing ways beyond the present phenomenological description with further experimental investigations.

References:

[1] I. Vurgaftman, J. R. Meyer, and L. R. Ram-Mohan, J. Appl. Phys., 89, 5816, (2001)

[2] I. Suemune, H. Sasakura, Y. Asano, H. Kumano, R. Inoue, K. Tanaka, T. Akazaki, and H. Takayanagi, IEICE Electron. Exp., 9, 1184, (2012)

[3] H. Sasakura, S. Kuramitsu, Y. Hayashi, K. Tanaka, T. Akazaki, E. Hanamura, R. Inoue, H. Takayanagi, Y. Asano, C. Hermannstaedter, H. Kumano, and I. Suemune, Phys. Rev. Lett. 107, 157403 (2011)

[4] S. S. Mou, H. Irie, Y. Asano, K. Akahane, H. Kurosawa, H. Nakajima, H. Kumano, M. Sasaki, and I. Suemune, IEEE J. Sel. Top. Quantum Electron. 21, 7900111 (2015)

[5] S. S. Mou, H. Irie, Y. Asano, K. Akahane, H. Nakajima, H. Kumano, M. Sasaki, A. Murayama, and I. Suemune, Phys. Rev. B 92, 035308 (2015)

[6] Y. Hayashi, K. Tanaka, T. Akazaki, M. Jo, H. Kumano, and I. Suemune, Appl. Phys. Express 1, 011701 (2008)

[7] I. Suemune, Y. Hayashi, S. Kuramitsu, K. Tanaka, T. Akazaki, H. Sasakura, R. Inoue, H. Takayanagi, Y. Asano, E. Hanamura, S. Odashima, and H. Kumano, Appl. Phys. Express 3, 054001 (2010)

[8] M. Tinkham, Introduction to Superconductivity. New York, USA, McGraw-Hill, (1975)

[9] L. Serrier-Garcia, J. C. Cuevas, T. Cren, C. Brun, V. Cherkez, F. Debontridder, D. Fokin, F. S. Bergeret, and D. Roditchev, Phys. Rev. Lett. 110, 157003 (2013)

[10] R. C. Dynes, V. Narayanamurti, and J. P. Garno, Phys. Rev. Lett. 41, 1509 (1978)

[11] V. Novotny and P. P. M. Meincke, J. Low Temp. Phys. 18, 147 (1975)

[12] J. A. van Dam, Y. V. Nazarov, E. P. A. M. Bakkers, S. De Franceschi, and L. P. Kouwenhoven, Nature (London) 442, 667 (2006)

[13] Y. Asano, I. Suemune, H. Takayanagi, and E. Hanamura, Phys. Rev. Lett., 103, 187001 (2009).

[14] X. Liu, K. Akahane, N. A. Jahan, N. Kobayashi, M. Sasaki, H. Kumano, and I. Suemune, Appl. Phys. Lett. 103, 061114, (2013)

[15] P. Hlobil and P. P. Orth, Phys. Rev. B 91, 205303 (2015)

[16] M. Bugajski and K. Reginski, Opto-Electron. Rev. 4, 84 (1996)

[17] S. S. Mou, H. Irie, Y. Asano, K. Akahane, H. Nakajima, H. Kumano, M. Sasaki, A. Murayama, and I. Suemune, J. Appl. Phys., 118, 073102, (2015)

[18] J. Seufert, R.Weigand, G. Bacher, T. Kuemmell, A. Forchel, K. Leonardi, and D. Hommel, Appl. Phys. Lett. 76, 1872, (2000)

Chapter 5

Cooper Pairs Recombination in InAs Quantum Dots: Time Resolved Measurements

In semiconductors, the characteristic charge carrier lifetime is highly dependent on the nature and dimensions of the materials and interfaces involved. Furthermore, surface effects, passivation and the energy transfer efficiency of sensitizers as well as the presence of dopants, impurities and defect sites can introduce significant variations in lifetime of charge carriers. Since the photoluminescence (PL) of semiconductors is a direct monitor of the charge carrier dynamics, the general methodology of time-resolved photoluminescence (TRPL) measurement via time-correlated single photon counting (TCSPC) and the periphery technology are highly suited for the analysis of the phenomena that determine fast charge carrier dynamics in a semiconductor.

In TRPL measurement, one measures the time between sample excitation by a pulsed laser and the arrival of the emitted photon at the detector. TRPL measurement via TCSPC requires a defined “start”, provided by the electronics operating the laser pulse, and a defined “stop” signal, realized by detection of a photon with single-photon sensitive detectors. The measurement of this time delay is repeated many times to account for the statistical nature of the emission from the experimental sample. The delay times are sorted into a histogram that plots the occurrence of emission over time after the excitation pulse.

In addition to CW PL spectroscopy, described in Chapter 4, TRPL spectroscopy was also performed on the prepared Ag-embedded Nb-superconductor/InAs QDs-based n-InGaAs heterostructure for investigating its optical properties more thoroughly. In this chapter, I discuss the details of TRPL spectroscopy of the prepared sample and the analysis of the obtained results.

5.1 Experimental Setup and Measurement Method

For luminescence measurement under pulsed excitation, the prepared sample was placed in a liquid-helium cooled cryostat and was excited with a mode-locked pulsed Titanium:Sapphire laser (operating at the wavelength of 770 nm) with 5-ps pulse width and 76 MHz repetition rate. The laser was focused onto one of the Nb/Ag embedded pillars on the surface with an objective lens (OL) of 0.4 numerical aperture (NA). PL emitted from InAs QDs was collected with the same OL and was dispersed by a double monochromator with 50-cm focal length and 300-grooves per-mm gratings and was detected with a liquid-nitrogen-cooled InGaAs-photodiode array detector.

For the TRPL measurement, emission from InAs QDs was coupled into a single-mode optical fiber (SMF) with an additional OL with NA of 0.25 and was directed into a superconducting single-photon detector (SSPD) by Single Quantum BV. The laser pulse was partially converted to an electrical pulse with a p-i-n photodiode and was used as the start signal, and signal from the SSPD was used as the stop signal of a time-to-amplitude converter (TAC). To spectrally select the QD emission, a 1570-nm band-pass filter (BPF) with ~20 nm bandwidth was inserted in the optical path before coupling to the SMF. Figure 5.1 shows the experimental setup of the TRPL measurement.

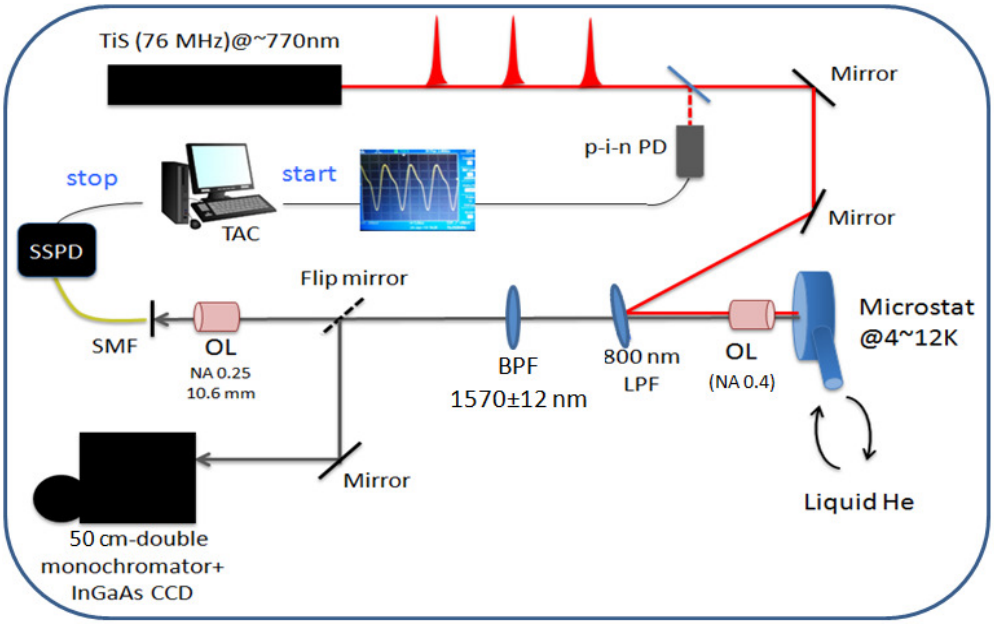

Fig. 5.1 Experimental setup for time resolved photoluminescence spectroscopy.

5.2 Spectral Measurements

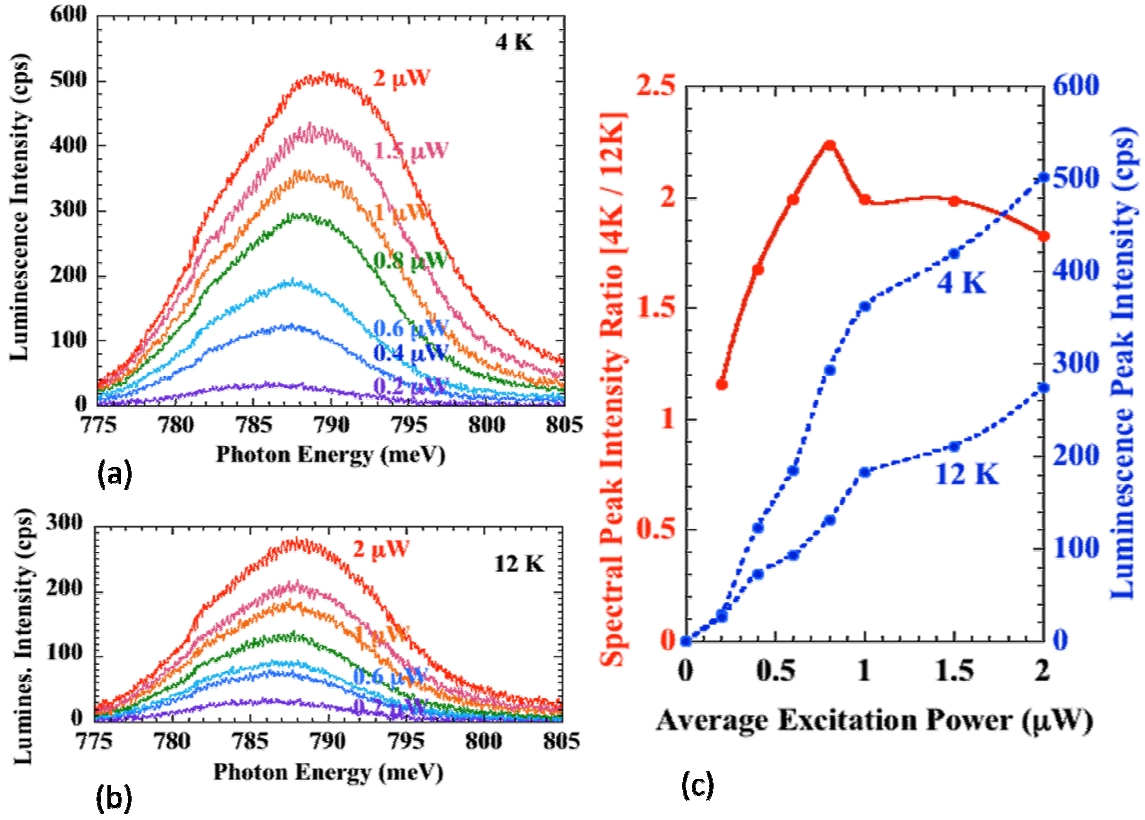

Fig. 5.2 (**a**) Excitation power dependence of time-averaged luminescence spectra measured at 4K under pulsed excitation. Time-averaged power is given for the pulsed-laser excitation (1 μW corresponds to the pulse peak power of 2.6 mW). cps represents photon counts per second. **(b)** Excitation power dependence of time-averaged luminescence spectra measured at 12K under pulsed excitation. **(c)** Excitation power dependence of peak intensity of time-averaged luminescence spectrum at 4K and 12K and the ratio of the peak intensities at 4K to 12 K.

Figures 5.2(a) and 5.2(b) show the excitation power dependence of InAs QD-emission luminescence spectra measured at 4K and 12K, respectively, on one of my prepared Ag-embedded Nb-superconductor/InAs QDs based n-InGaAs heterostructure pillars with the diameter of 1.5 μm [1]. The excitation power is given with the time-averaged value for the pulsed excitation. It is observed that the QD luminescence spectra are slightly blue shifted for

the higher excitation. Although the spectra are not much temperature dependent, the luminescence intensity measured at 4K is almost double of that at 12 K. The peak intensity measured at 4K and 12K and the ratio of the two (4K / 12K) is plotted against the excitation power in Fig. 5.2(c). There is a saturation behavior observed around the excitation power of 1 μW, which is attributed to the filling of QDs' lowest energy states with increasing excitation power (hole filling in the present n-type heterostructure). It is clearly seen that the luminescence intensity measured at 4K is highly enhanced by two times. This substantial enhancement below the SC critical temperature of T_C ~9.09 K reproduces the luminescence enhancement observed in my continuous-wave (CW) measurement [2], described in Chapter 4, and in previously measured QW structures [3, 4].

My next step is to focus on TRPL measurements to confirm the role of Cooper-pair recombination for the luminescence enhancement. For this purpose, an analytical method is proposed in the next section, to identify the contribution of Cooper-pair recombination in InAs QDs quantitatively.

5.3 Analytical Method

As discussed in Chapter 2, the photon emission from the InAs QDs is regulated by minority holes in the present n-type heterostructure. Hence luminescence decay is regulated by the lifetime of minority holes. A lifetime generally consists of two parts: radiative lifetime τ_{rad} and non-radiative lifetime τ_{nonrad}. To distinguish the terms below and above T_C, the subscript of L and U will be used, respectively. For temperature above T_C, the lifetime is given by,

$$\tau_U^{-1} = \tau_{rad,U}^{-1} + \tau_{nonrad,U}^{-1}, \text{ when } T = T_U > T_C \qquad (5.1)$$

For temperature below T_C, the additional Cooper-pair recombination term is included and the lifetime is given by,

$$\tau_L^{-1} = \tau_{rad,L}^{-1} + \tau_{nonrad,L}^{-1} + \tau_{super}^{-1}, \text{ when } T = T_L \leq T_C \qquad (5.2)$$

where τ_{super} is the superconducting term due to the Cooper-pair recombination. Measured luminescence intensity is proportional to the internal quantum efficiency (IQE) and is given by,

$$I_{Lum,U} / I_0 = \eta_{ext}\eta_{int,U} = \frac{\tau_{rad,U}^{-1}}{\tau_{nonrad,U}^{-1} + \tau_{rad,U}^{-1}} = \frac{\tau_{rad,U}^{-1}}{\tau_U^{-1}}, \quad T = T_U > T_C \qquad (5.3)$$

and

$$I_{Lum,L} / I_0 = \eta_{ext}\eta_{int,L} = \frac{\tau_{rad,L}^{-1} + \tau_{super}^{-1}}{\tau_{nonrad,L}^{-1} + \tau_{rad,L}^{-1} + \tau_{super}^{-1}}$$

$$= \frac{\tau_{rad,L}^{-1} + \tau_{super}^{-1}}{\tau_L^{-1}}, \quad T = T_L \leq T_C \qquad (5.4)$$

where I_{Lum} is the measured luminescence intensity and η_{int} is the IQE. η_{ext} is the external collection efficiency of photons emitted from InAs QDs and is temperature-independent. I_0 is

the luminescence intensity in the case of 100% efficiency. Normal radiative lifetime in InAs QDs remains almost constant in the low-temperature range studied in this work (4 K ~ 12 K) [5]. Hence it can be considered that,

$$\tau_{\mathrm{rad,U}}^{-1} = \tau_{\mathrm{rad,L}}^{-1} \equiv \tau_{\mathrm{rad}}^{-1}.$$

Since electrons very close to the electron Fermi level are condensed in the superconducting density of states (SC DOS) based on the Bardeen Cooper Schrieffer (BCS) theory [6], this assumption is rationalized in the present highly n-type doped sample. Therefore, taking the ratio of the luminescence intensities measured below and above SC T_C, T_L and T_U, as R_{Lum} (= $I_{Lum,L}/I_{Lum,U}$), it is obtained as follows,

$$R_{Lum} = (1 + \tau_{\mathrm{super}}^{-1} / \tau_{\mathrm{rad}}^{-1}) \frac{\tau_{\mathrm{U}}^{-1}}{\tau_{\mathrm{L}}^{-1}}. \qquad (5.5)$$

Taking the ratio of the decay time constants measured at T_L and T_U as $R_{lifetime}$ ($= \frac{\tau_{\mathrm{U}}^{-1}}{\tau_{\mathrm{L}}^{-1}}$), the ratio of the superconductive (Cooper-pair) to normal radiative recombination rates is given by,

$$\tau_{\mathrm{super}}^{-1} / \tau_{\mathrm{rad}}^{-1} = R_{\mathrm{Lum}} / R_{\mathrm{lifetime}} - 1. \qquad (5.6)$$

As it can be seen from equation (5.6), the ratio of superconductive to normal radiative recombination rates is uniquely determined by this equation using the known parameters that could be directly obtained from experimentally measured values. In the total photon emission process from the QDs, the numerator in the left term of Eq. (5.6) gives the contribution from electron Cooper pairs, and the denominator gives the one from normal electrons.

From Eqs. (5.1) – (5.4), it is also possible to study the τ_{nonrad} term (nonradiative recombination), but it needs additional information about how it depends on temperature.

5.4 Time Resolved Luminescence Measurements

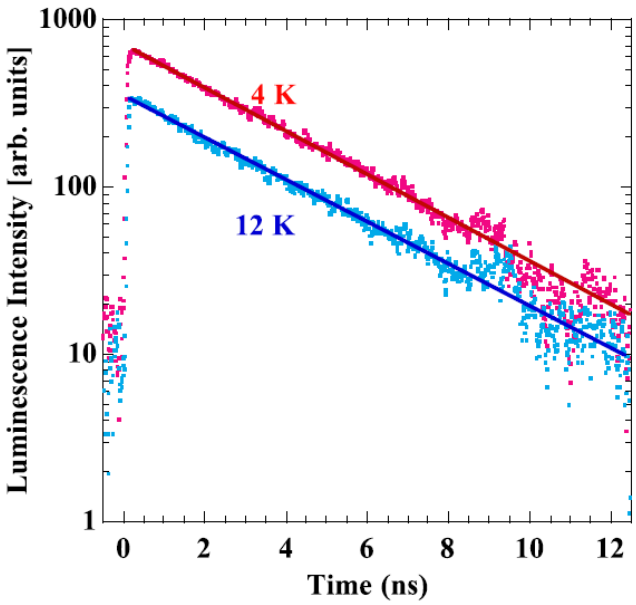

Fig. 5.3 Time decay of luminescence peak intensity from InAs QD emission measured at the wavelength of 1570 nm (790 meV) with the bandwidth of 20 nm (10.1 meV). The average excitation power is 0.8 μW (pulse peak power is 2.1 mW). The solid lines are the fitting curves obtained with a single exponential function.

The transient decay of the QD luminescence from one of the Ag/Nb-embedded heterostructure pillars was measured below and above SC T_C, at 4K and 12K, respectively, with the average excitation power of 0.8 μW and is shown in Fig. 5.3. The measured decay is fitted by a single exponential function and the results are shown with the solid lines. The fitting results in the decay time constant s of 3.01 ns at 4K and 3.41 ns at 12 K.

The measured temperature dependence of the transient QD PL peak intensity and the luminescence decay time constant is shown in Fig. 5.4. The luminescence intensity shows sharp increase below SC T_C of 9.09 K. This well reproduces my previous observation of PL

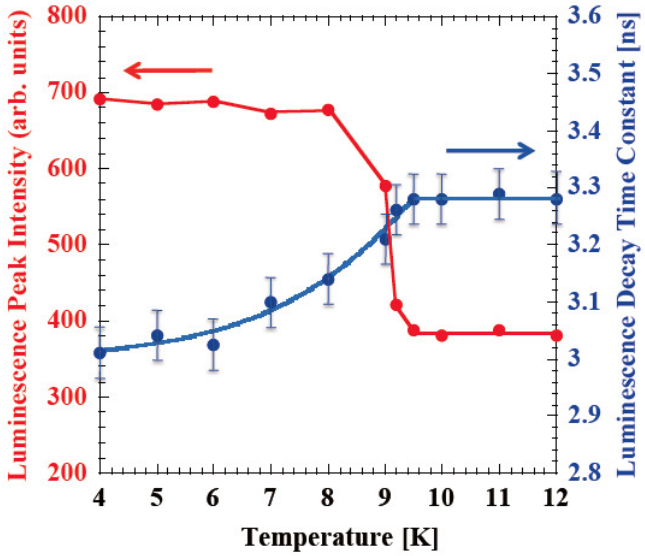

Fig. 5.4 Temperature dependence of transient luminescence peak intensity and luminescence decay time constant with error bars measured at an average excitation power of 0.8 μW.

enhancement in CW PL spectroscopy, discussed in the previous chapter, and in SC-LEDs [3, 4]. Above T_C the decay time constant remains the same, but below T_C it shows clear decrease with temperature. This behavior also well reproduces the previous observation of decrease of the electroluminescence decay time constant in SC-LEDs [7, 8]. These correlations of both the luminescence intensity and the decay time constant to the SC critical temperature (T_C) are the clear evidences that the observed phenomenon is based on the Cooper-pair recombination in InAs QDs penetrated from the Nb superconductor.

The ratio of the superconductive to normal radiative recombination rates has been studied by employing the measured data in Fig. 5.4. As it can be observed from Fig. 5.4 that both the luminescence intensity and the decay time constant remain almost constant above T_C, the result is not much dependent on the selection of temperature above T_C (T_U) in Eqs. (5.1) - (5.4). In this case, T_U was set to the measured highest temperature of 12 K. The result is shown with closed circles in Fig. 5.5 and is further studied theoretically.

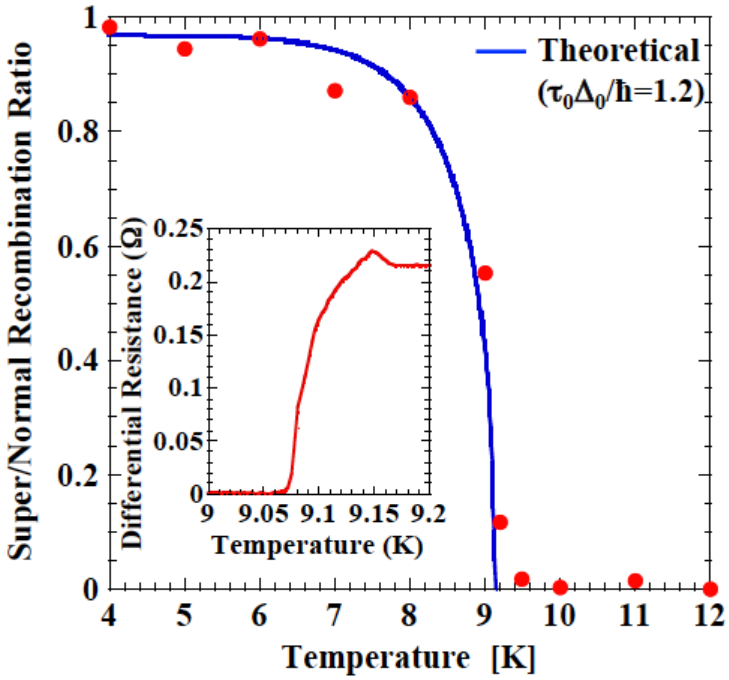

Fig. 5.5 Temperature dependence of the ratio of superconductive to normal radiative recombination rate. Closed circles are data from measurements. The solid line is theoretical based on Ref. 9. Δ_0 is half of the SC gap (pair potential) at zero temperature and τ_0 is the relaxation time due to elastic impurity scattering. The inset graph is the temperature dependence of the differential resistance measured on the evaporated Nb layer expanded near T_C.

The theory on the Cooper-pair luminescence presented by Y. Asano, I. Suemune et al. is based on the second-order perturbation theory for electron-photon interaction [9], and they calculated the time-averaged expectation value of the number of emitted photons. The superconductivity effect is included through the Bogoliubov transformation from operators for electrons to those for Bogoliubov quasiparticles [10]. In Ref. 9, two cases of finite relaxation time was considered, which originates from scattering of electron Cooper pairs penetrated into the n-type semiconductor. One is elastic impurity scattering and the other is inelastic scattering such as electron-phonon scattering and repulsive electron-electron scattering. Both cases resulted in similar temperature-dependent luminescence enhancement below T_C. In Fig. 5.5, I fitted the data with the case of elastic impurity scattering. The solid

line is for $\Delta_0\tau_0/\hbar = 1.2$, where Δ_0 is half of the SC gap at zero temperature, τ_0 is the relaxation time due to elastic impurity scattering, and $\hbar$ is the Planck's constant divided by 2π. The measured T_C of Nb of my sample is 9.09 K. However, a transient temperature range appears as is observed in the inset of Fig. 5.5, and the differential resistance reaches the maximum at 9.15 K. Since T_C of intrinsic Nb is known to be 9.26 ± 0.01 K [11], this transient behavior implies that SC regions survive in the Nb layer inhomogeneously in the temperature range of 9.09 –9.15 K. Therefore, the T_C is set as 9.15 K in my theoretical calculation and the measured superconducting Cooper-pair luminescence enhancement was fitted very nicely, as shown in Fig. 5.5.

5.5 Discussion

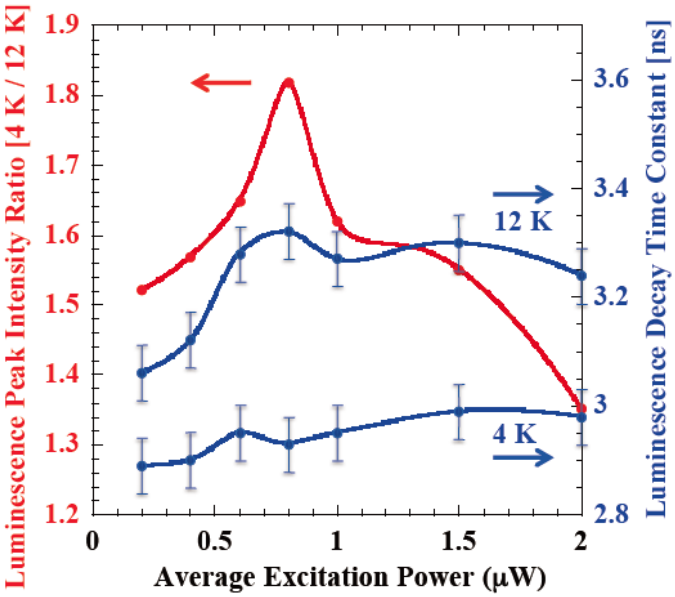

Fig. 5.6 Excitation power dependence of the ratio of the transient QD luminescence peak intensities at 4 K to that at 12 K (left axis) and the luminescence decay time constants with error bars at 4 K and 12 K (right axis).

The results of excitation power dependence of the transient properties shown in Fig. 5.3 are summarized in Fig. 5.6. The measured decay time constants are shorter at 4K in comparison to 12 K, but they show relatively weak excitation power dependence. On the other hand, the ratio of the transient luminescence peak intensities measured at 4K and 12K exhibits relatively sharp peak at the average excitation power of 0.8 μW. Similar characteristics is observed with the time-averaged spectral peak intensity ratio shown in Fig. 5.2(c). The ratios observed with the average excitation power of 1.5 and 2 μW show a different tendency between the two measurements. This is attributed to the QD-state population saturation of photoexcited minority holes as is evident from the luminescence saturation shown in Fig. 5.2(c).

Employing the measured data in Fig. 5.6, the ratio of the superconductive to normal radiative recombination rates has been studied with the method presented in Section 5.3 and the result is shown in Fig. 5.7. The ratio shows the sharp peak at the average excitation power of 0.8 μW, indicating the highest enhancement of the SC Cooper-pair recombination at that excitation power.

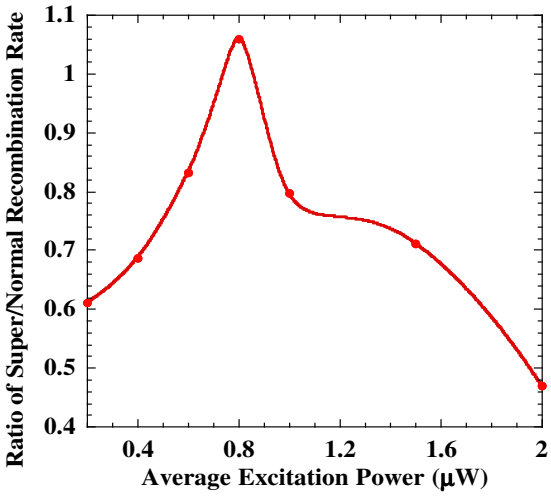

Fig. 5.7 Average excitation power dependence of the ratio of Cooper-pair superconductive to normal radiative recombination rates.

In all the samples, the SC enhancement has been reproducibly observed around the photon energy of 790 meV as shown in Fig. 5.2. This is because of the uniform n-type doping in the present InGaAs-based heterostructure, where the conduction-band Fermi level is almost uniform and common in the grown sample. In some high-quality samples, a “sharp edge” in the luminescence spectra below T_C has been observed [12]. I interpreted this luminescence sharp edge as reflection of the sharp SC-DOS near the SC gap. Below T_C, electrons near the Fermi level form Cooper pairs and are condensed to the SC-DOS, and the SC gap opens near the electron Fermi level. Then QDs, whose conduction-band lowest energy states are near resonance with the energy of the SC-DOS, experience enhanced photon emission by the Cooper-pair recombination [2, 12].

Regarding the excitation power dependence, the minority-hole population in the valence-band lowest QD states change with the excitation power. When the excitation remains low, the hole population among QDs is determined mainly by the capture process of photo-generated carriers at low temperature. It has been presumed that dominantly luminescent QDs at this stage are those of which conduction-band energy states are off resonant to the SC-DOS. With the higher excitation, population of the lowest energy states of larger dots are saturated, and the population of their excited states and carrier transfer to smaller QDs with higher QD-state energies happen through coupled excited states [13]. Then, when the conduction-band QD-state energies of dominantly luminescent QDs come to near resonance with the SC-DOS, the SC recombination rate reaches the maximum as shown in Fig. 5.7. This results in the observed excitation power dependence with the peak excitation power at 0.8 μW.

In Fig. 5.5, I calculated the theoretical curve numerically. In Ref. 9, an analytical formula of the time averaged expectation value of the number of emitted photons was derived for $\Delta_0\tau_0/\hbar < 1$, i.e., for the case of higher scattering probability. The major term regulating the temperature dependence in this formula is Δ^2/T, and the enhancement is proportional to the square of half the SC gap at a given temperature T and inversely proportional to T [9]. The observed enhancement in the previous SC-LEDs could be fitted with this analytical formula [4, 7, 8, 14]. But the Δ^2/T dependence shows more slowly varying temperature dependence than that shown in Fig. 5.5 and can be approximated for $\Delta_0\tau_0/\hbar < 0.2$.

The parameter $\Delta_0\tau_0/\hbar \geq 1$ in Fig. 5.5 indicates lower scattering probability. $\Delta_0\tau_0/\hbar < 1$ in the previous SC-LEDs indicated that higher scattering probability prevents coherent Cooper-pair enhancement of radiative recombination. This results in the milder temperature dependence of luminescence enhancement below T_C. Therefore, I attribute the sharp increase of the luminescence enhancement below T_C to the lower scattering probability of Cooper pairs in my present sample. The difference between the SC-LED samples and my InAs QD-based heterostructure sample is that the previous SC-LEDs were grown on (001) InP substrate with metalorganic chemical vapor deposition (MOCVD), while the present QD-based sample was

grown on (311)B InP substrate with MBE. The other difference is that most of the previous SC-LEDs were doped n-type up to $5x10^{18}$ cm^{-3} [3, 7], while the present sample was doped $1x10^{18}$ cm^{-3}. In principle, the higher electron concentration extends the coherence length as discussed in Chapter 2, but the higher impurity concentration may increase the scattering probability.

References:

[1] S. S. Mou, H. Irie, Y. Asano, K. Akahane, H. Nakajima, H. Kumano, M. Sasaki, A. Murayama, and I. Suemune, J. Appl. Phys., 118, 073102, (2015)

[2] S. S. Mou, H. Irie, Y. Asano, K. Akahane, H. Nakajima, H. Kumano, M. Sasaki, A. Murayama, and I. Suemune, Phys. Rev. B 92, 035308 (2015)

[3] Y. Hayashi, K. Tanaka, T. Akazaki, M. Jo, H. Kumano, and I. Suemune, Appl. Phys. Express 1, 011701 (2008)

[4] I. Suemune, Y. Hayashi, S. Kuramitsu, K. Tanaka, T. Akazaki, H. Sasakura, R. Inoue, H. Takayanagi, Y. Asano, E. Hanamura, S. Odashima, and H. Kumano, Appl. Phys. Express 3, 054001 (2010)

[5] N. A. Jahan, C. Hermannstaedter, J.-H. Huh, H. Sasakura, T. J. Rotter, P. Ahirwar, G. Balakrishnan, K. Akahane, M. Sasaki, H. Kumano, and I. Suemune, J. Appl. Phys. 113, 033506 (2013)

[6] M. Tinkham, Introduction to Superconductivity, 2nd ed. (Dover, New York, 2004)

[7] H. Sasakura, S. Kuramitsu, Y. Hayashi, K. Tanaka, T. Akazaki, E. Hanamura, R. Inoue, H. Takayanagi, Y. Asano, C. Hermannstaedter, H. Kumano, and I. Suemune, Phys. Rev. Lett. 107, 157403 (2011)

[8] I. Suemune, H. Sasakura, Y. Asano, H. Kumano, R. Inoue, K. Tanaka, T. Akazaki, and H. Takayanagi, IEICE Electron. Express 9, 1184 (2012)

[9] Y. Asano, I. Suemune, H. Takayanagi, and E. Hanamura, Phys. Rev. Lett. 103, 187001 (2009)

[10] J. Unterhinninghofen, D. Manske, and A. Knorr, Phys. Rev. B 77, 180509(R) (2008)

[11] V. Novotny and P. P. M. Meincke, J. Low Temp. Phys. 18, 147 (1975)

[12] S. S. Mou, H. Irie, Y. Asano, K. Akahane, H. Kurosawa, H. Nakajima, H. Kumano, M. Sasaki, and I. Suemune, IEEE J. Sel. Top. Quantum Electron. 21, 7900111 (2015)

[13] C. Hermannstaedter, N. A. Jahan, J.-H. Huh, H. Sasakura, K. Akahane, M. Sasaki, and I. Suemune, New J. Phys. 14, 023037 (2012)

[14] I. Suemune, H. Sasakura, Y. Hayashi, K. Tanaka, T. Akazaki, Y. Asano, R. Inoue, H. Takayanagi, E. Hanamura, J.-H. Huh, C. Hermannstaedter, S. Odashima, and H. Kumano, Jpn. J. Appl. Phys., Part 1 51, 010114 (2012)

Chapter 6

Conclusion

6.1 Summary of The Work

In this work, I have studied luminescence spectra of InAs quantum dots (QDs) in an n-type InGaAs-based heterostructure grown on InP (311)B substrate, where electron Cooper pairs penetrate from an adjacent Nb superconductor layer with the proximity effect [1]. I have experimentally demonstrated the injection and recombination of Cooper pairs in InAs QDs employing continuous-wave (CW) and time-resolved photoluminescence (PL) spectroscopy measurements.

Ag/Nb embedded nanopillars were fabricated with the InAs-QD-based heterostructure sample. With CW PL spectroscopy, Major enhancement of QD luminescence intensity below superconducting critical temperature (SC T_C) of Nb was observed which evidenced the penetration and recombination of Cooper pairs in InAs QDs. This reproduced the Cooper-pair-based luminescence enhancement previously observed in SC-LEDs [2, 3]. It is also observed that the peak intensity of QD luminescence spectra reflects the distribution of QD sizes and therefore of the QD discrete energy states, and below SC T_C QDs nearly in resonance with the superconducting density of states are enhanced in their emission.

A sharp edge was observed in luminescence spectra of InAs QDs with CW spectroscopy, at the photon energy of ~790 meV below the SC T_C of Nb. I have explained the observed sharp edge in the luminescence spectra by considering opening of the SC gap and modification of the band structure to the superconducting density of states (SC DOS) near the electron Fermi level in the n-type semiconductor heterostructure. I demonstrated that the observation of the sharp edge in the luminescence spectra of InAs QDs is sensitive to the quasiparticle lifetime broadening.

With time-resolved measurements of QD luminescence around the wavelength of 1570 nm, I demonstrated abrupt luminescence intensity enhancement and reduction of luminescence

decay time constant below SC T_C of Nb, which reproduced luminescence of Cooper pairs observed in my CW measurements and in the previously studied QW-based SC-LEDs [4, 5].

I proposed a deterministic method to find the contribution of Cooper-pair recombination in InAs QDs quantitatively. I also studied the measured temperature dependence of the Cooper-pair recombination theoretically and demonstrated its excellent agreement of the measured results with the theory of Cooper-pair luminescence based on the second-order perturbation theory for electron-photon interaction. I have also discussed the difference of the temperature dependence between my QD-based heterostructure samples and the previously measured QW-based samples.

In conclusion, this work presents detailed experimental and analytical studies of the luminescence properties of the n-type-doped InAs-QD-based heterostructure/Nb superconductor system. I believe that my findings provide useful information which opens a way to further study the proximity effect of superconductivity with the optical techniques and offers the possibility to find new physics related to superconductivity and optoelectronics. This work also analyzes the InAs QD-based heterostructure system's performance and advancement towards realizing superconductor-based QD light emitting diode (SQLED) for generating quantum entangled photon pairs (QEPPs) [6].

6.2 Future Prospect

The present work confirmed the penetration and recombination of Cooper pairs in InAs QDs, which fulfilled the most important prerequisite for realizing the superconductor-based QD light emitting diode (SQLED) to generate on-demand quantum entangled photon pairs (QEPP) [6]. The key issue of SQLED theory is to control the photon-pair generation process by regulating the number of holes involved in the recombination with Cooper pairs, and this is possible by the use of the ground state of the QD valence band employing the Pauli's exclusion principle, as shown in Fig. 6.1 [7]. Therefore, this technique is expected to lead to the generation of on-demand QEPP.

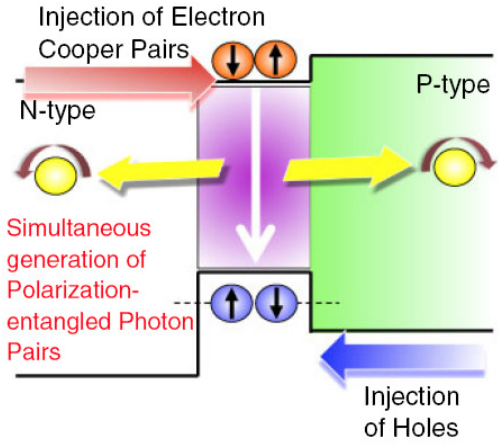

Fig. 6.1 Fundamental band diagram and operation principle of SQLED [7]

Having ensured the Cooper pairs recombination in InAs QDs, the remaining issue to pursue is the demonstration of photon bunching of the emitted photons to prove the QEPP generation. This will be possible by the photon correlation measurements of photons emitted from a single QD in the Ag/Nb-superconductor embedded InAs QD-based heterostructure system and the study is in progress.

References:

[1] P. G. de Gennes, Superconductivity of Metals and Alloys (Boulder: Westview Press, 1999)

[2] Y. Hayashi, K. Tanaka, T. Akazaki, M. Jo, H. Kumano, and I. Suemune, Appl. Phys. Express 1, 011701 (2008)

[3] I. Suemune, Y. Hayashi, S. Kuramitsu, K. Tanaka, T. Akazaki, H. Sasakura, R. Inoue, H. Takayanagi, Y. Asano, E. Hanamura, S. Odashima, and H. Kumano, Appl. Phys. Express 3, 054001 (2010)

[4] H. Sasakura, S. Kuramitsu, Y. Hayashi, K. Tanaka, T. Akazaki, E. Hanamura, R. Inoue, H. Takayanagi, Y. Asano, C. Hermannstaedter, H. Kumano, and I. Suemune, Phys. Rev. Lett. 107, 157403 (2011)

[5] I. Suemune, H. Sasakura, Y. Asano, H. Kumano, R. Inoue, K. Tanaka, T. Akazaki, and H. Takayanagi, IEICE Electron. Express 9, 1184 (2012)

[6] I. Suemune, T. Akazaki, K. Tanaka, M. Jo, K. Uesugi, M. Endo, H. Kumano, E. Hanamura, H. Takayanagi, M. Yamanishi, and H. Kan, Jpn. J. Appl. Phys., Part 1 45, 9264 (2006)

[7] I. Suemune, H. Sasakura, Y. Hayashi, K. Tanaka, T. Akazaki, Y. Asano, R. Inoue, H. Takayanagi, E. Hanamura, J.-H. Huh, C. Hermannstaedter, S. Odashima, and H. Kumano, Jpn. J. Appl. Phys., Part 1 51, 010114 (2012)

List of Publications in Refereed Journals

1. "Time-resolved measurements of Cooper-pair radiative recombination in InAs quantum dots"

Authors: **Sinthia Shabnam Mou**, H. Irie, Y. Asano, K. Akahane, H. Nakajima, H. Kumano, M. Sasaki, A. Murayama, and I. Suemune

Journal**:** Journal of Applied Physics, Volume 118, 073102, August 2015

2. "Optical observation of superconducting density of states in luminescence spectra of InAs quantum dots"

Authors: **Sinthia Shabnam Mou,** H. Irie, Y. Asano, K. Akahane, H. Nakajima, H. Kumano, M. Sasaki, A. Murayama, and I. Suemune

Journal: Physical Review B, Volume 92, 035308, July 2015

3. "Superconducting Light-emitting Diodes"

Authors: **Sinthia Shabnam Mou,** Hiroshi Irie, Y. Asano, Kouichi Akahane, Hiroyuki Kurosawa, Hideaki Nakajima, Hidekazu Kumano, Masahide Sasaki, and Ikuo Suemune

Journal: IEEE Journal of Selected Topics in Quantum Electronics, Volume 21, No.2, March 2015

List of Publications in Conferences and Symposiums

1. "Enhancement of Luminescence in InAs Quantum Dots employing Cooper-pair Recombination"

Authors: **Sinthia Shabnam Mou**, Hiroshi Irie, Kouichi Akahane, Hiroyuki Kurosawa, Hideaki Nakajima, Hidekazu Kumano, Masahide Sasaki, and Ikuo Suemune

Symposium: The 75th JSAP Autumn Meeting 2014, Sep 17-20, 2014, Sapporo, Hokkaido, Japan

2. "Signature of Superconducting Density of States in Luminescence Spectra of InAs Quantum Dots"

Authors: **Sinthia Shabnam Mou**, Hiroshi Irie, Kouichi Akahane, Hiroyuki Kurosawa, Hideaki Nakajima, Hidekazu Kumano, Masahide Sasaki, and Ikuo Suemune

Symposium: International Conference on Solid State Devices and Materials, Sep 8-11, 2014, Tsukuba, Japan

3. "Luminescence of Cooper Pairs in an InAs Quantum Dot Heterostructure"

Authors: **Sinthia Shabnam Mou**, Hiroyuki Kurosawa, Hiroshi Irie, Kouichi Akahane, Satoru Odashima, Hidekazu Kumano, Masahide Sasaki, and Ikuo Suemune

Symposium: Compound Semiconductor Week 2014, May 11-15, 2014, Montpellier, France

4. "Possibility of Entangled Photon Pair Generation in InAs Quantum Dot Heterostructure employing Cooper-pair Recombination"

Authors: Sinthia Shabnam Mou, H. Takeda, Kouichi Akahane, Masahide Sasaki, Hiroshi Irie, Hidekazu Kumano, and Ikuo Suemune

Symposium**:** The 49th JSAP conference, Dec 9-10, 2013, Sapporo, Hokkaido, Japan

5. "Study of Cooper-pair Recombination in InAs Quantum Dot Heterostructure"

Authors: **Sinthia Shabnam Mou**, H. Takeda, Kouichi Akahane, Masahide Sasaki, Hiroshi Irie, Hidekazu Kumano, and Ikuo Suemune

Symposium: International Symposium on Nanoscale Transport and Technology, Nov 26-29, 2013, Atsugi, Kanagawa, Japan.